RHDHV

South Bay, Scarborough

Beach Sand Tracking Study

April 2015

Partrac Ltd
440 Baltic Chambers
50 Wellington Street
Glasgow
G2 6HJ

+44 (0) 141 202 0644
info@partrac.com
www.partrac.com

DOCUMENT CONTROL

Version History					
Version	Date	Prepared by	Reviewed by	Approved by	Approved as
V01	24/04/2015	M Wright J Poleykett K Black	K Black	K Black	Draft
V02	06/05/2015	M Wright	K Black	K Black	Final

Changes from the Previous Version	
V02	Updated following client comment to be issued as Final

Recipient	Distribution Method		
	Paper (copies)	PDF	Online
Nick Cooper – RHDHV		X	
Robin Siddle – Scarborough BC		X	

Holders of controlled copies will automatically be provided with subsequent approved versions of this document when they become available.

CONTENTS

1. INTRODUCTION **8**
1.1 Background 8
1.2 Study Aims 9
1.3 Dual Signature Tracers 10
2. TRACER DESIGN, MANUFACTURE AND TESTING **12**
2.1 Introduction 12
2.2 Beach Sand Sedimentology 12
2.3 Tracer Design and Hydraulic Characterisation 14
2.4 Summary Characteristics 19
3. SURVEY METHODOLOGY **20**
3.1 Introduction 20
3.2 Tracer Preparation and Introduction 20
3.3 Navigation & Positioning 25
3.4 Sampling 25
3.5 Supporting Oceanographic Data 27
4. TRACER ENUMERATION **28**
4.1 Introduction 28
4.2 Sample Preparation 28
4.3 Gilden Photonics™ Fluorimeters 29
4.4 Methodology 29
5. CALIBRATION AND QUALITY CONTROL **33**
5.1 Dose Response Curves 33
5.2 Minimum Resolvable Mass (MRM) 33
5.3 QC Data – Periodic Testing of Blanks 36
5.4 Testing of Blind Samples 37
6. RESULTS AND DISCUSSION **38**
6.1 Tracer Dry Mass Data 38
6.2 Magnetic Susceptibility Data 48
7. CONCLUDING REMARKS **55**
8. REFERENCES **56**

9. APPENDIX I GILDEN PHOTONICS FLUOROSENS FLUORIMETER TECHNICAL SPECIFICATION 58

10. APPENDIX II TRACER DATA 59

LIST OF FIGURES

Figure 1. postulated tidal current pathways in the nearshore region of Scarborough South Bay 9

Figure 2. Comparison of the particle size distribution of the manufactured tracer and native beach sediment. 15

Figure 3. Photograph of the green tracer mixed with native beach sand at a concentration of 0.001 g cm^{-2} (left) and 0.185 g cm^{-2} (right) under blue light illumination (UV-A~395 nm)........17

Figure 4. Emission – excitation spectra for the green tracer pigment. 18

Figure 5. Deployment of the Tracer Material at Deployment Zone 2 21

Figure 6. Deployment of the Tracer Material at Deployment Zone 2 21

Figure 7. Deployment of the Tracer Material at Deployment Zone 3 22

Figure 8. Deployment of the Tracer Material at Deployment Zone 3 22

Figure 9. Location of tracer material Deployment Zones and of the entire sample set collected for the six sampling campaigns. 24

Figure 10. Trimble R4 GNSS RTK base and rover system used for positioning during the study. 25

Figure 11. The Fluorosens laboratory fluorimeter. 29

Figure 12. Dose response curves for Low, Intermediate and High sediment volume for all the samples collected. In practise the point concentration values on the x-axis are interchangeable with the corresponding tracer dry mass of each curve. 35

Figure 13. Geospatial distribution of tracer dry mass (g m^{-2}) ~24 hours after injection. 39

Figure 14. Geospatial distribution of tracer dry mass (g m^{-2}) ~48 hours after injection. 40

Figure 15. Geospatial distribution of tracer dry mass (g m^{-2}) ~72 hours after injection. 41

Figure 16. Geospatial distribution of tracer dry mass (g m^{-2}) ~7 days after injection. 42

Figure 17. Geospatial distribution of tracer dry mass (g m^{-2}) ~14 days (semi-lunar cycle) after injection. 43

Figure 18. Geospatial distribution of tracer dry mass (g m^{-2}) 54 days after injection. 44

Figure 19. Distribution of surface low frequency magnetic susceptibility (χ_{LF}) at Deployment Zone 1 pre – injection of tracer (background), post injection of tracer and following the first wave event..........................51

Figure 20. The low frequency magnetic susceptibility (χ_{LF}) of Deployment Zone 2 pre – injection of tracer (background), post injection of tracer and following the first wave event. 52

Figure 21. The low frequency magnetic susceptibility (χ_{LF}) of Deployment Zone 3 pre - injection of tracer (background), post injection of tracer and following the first wave event. 53

LIST OF TABLES

Table 1: Summary particle size data for beach material samples collected from various locations. LB=lower beach; MB=mid-beach; HB=high beach....13

Table 2: Summary magnetic fraction of the native sediment. 14

Table 3: Low frequency mass specific magnetic susceptibility (χ_{LF}) of the tracer and a quartzitic beach sand provided as a comparison..............................16

Table 4: The percentage of tracer particles that are magnetic. 16

Table 5: Excitation and emission wavelengths for green tracer......................18

Table 6: Summary of the characteristics of the native beach sand and tracer. 19

Table 7: Date and location of deployment zones, location fixed from upper foreshore southern edge of zone (SW corner). Coordinates are OSGB National Grid)..23

Table 8 Summary of r^2 values of the dose response curves for differing background sediment loadings...33

Table 9 Summary of MRM values for each dose response curve.....................33

Table 10: **Periodic testing of laboratory blanks for mono-colour (green) tracer dye.** 36

Table 11: Periodic testing of blind samples (green tracer). 37

Table 12: Details of the inshore wave climatology from the CCO Scarborough wave buoy through the dominant portion of the study (i.e. to 19th December, 2014)......46

Table 13: Raw magnetic susceptibility (χLF) values. 49

1. INTRODUCTION

The movement of energy and materials within the geosphere is a fundamental attribute of the Earth system. Processes of atmospheric and hydrologic weathering erode the surface rocks and soils, and overland, fluvial and marine currents act to transport and redistribute particles. Anthropogenically produced particles, such as soot, urban contaminants, mine tailings and radionuclides are also subject to the same transport and re-distribution processes. An understanding of the mechanisms and processes of re-distribution is necessary to understanding both the natural geological consequences of erosion, and the transport and fate of anthropogenically produced particles (contaminants).

'**Particle tracking**', or as it is sometimes referred to in the geological sciences 'sediment tracing' or 'sediment tracking', offers a unique methodology with which to track the movement through space and time of environmental particulates. Utilising this methodology, information can be garnered into source – sink relationships, the nature and location of the transport pathway[s] and the rate of transport. It is a relatively straightforward, practical methodology which involves the introduction of particulate tracers into the environment (water body, sewer, beach etc.) labelled with one or more signatures in order that they may be unequivocally identified following release (McComb and Black, 2005; Forsyth, 2000). Sampling at strategic locations and timings is used to collect tracer which is then returned to the laboratory for analysis. Measurable and uniquely identifiable signatures have in the past included the use of radioactive tracers (Courtois and Monaco 1969; Heathershaw and Carr 1978) and Rare Earth elements (Spencer, in press), fluorescent coated sands (Vila-Conjeco *et al*., 2004); fluorescent silts (Sarma & Iya, 1960; Draaijer *et al*. (1984); Louisse *et al*. (1986)). However, radioactive tracers are now considered unacceptable on economic and environmental grounds. Synthetic, polymer-based, tracers have also been developed (e.g. Black and McComb, 2005). Black *et al*. (2007) provide a comprehensive overview of the historic evolution of these differing approaches to the present day. Regardless of the tracer deployed, the approach to any soil or sediment project is largely the same.

1.1 Background

Dr Nick Cooper (Royal Haskoning DHV, Newcastle) approached Partrac Ltd to discuss a commercial opportunity to investigate tracking the movement of beach sand on the shoreface on the Scarborough (North Yorkshire), South Bay frontage. There are issues at this location associated with the return of excavated/recycled beach material to its source, due to a hypothesised northward current recirculation (see Figure 1) at the northward end of the bay. This is in the opposite direction to the general North to South trending longshore drift direction along this coastline. The return of the material leads to localised accumulation and build-up of sand which periodically overtops the wall at the back of the beach and is deposited on the promenade road. There is also interest to know if material is transported to a shallow offshore bar, and if it is, whether there is ensuing transport northeastward into the area of the Scarborough Harbour mouth infilling the navigational access channel.

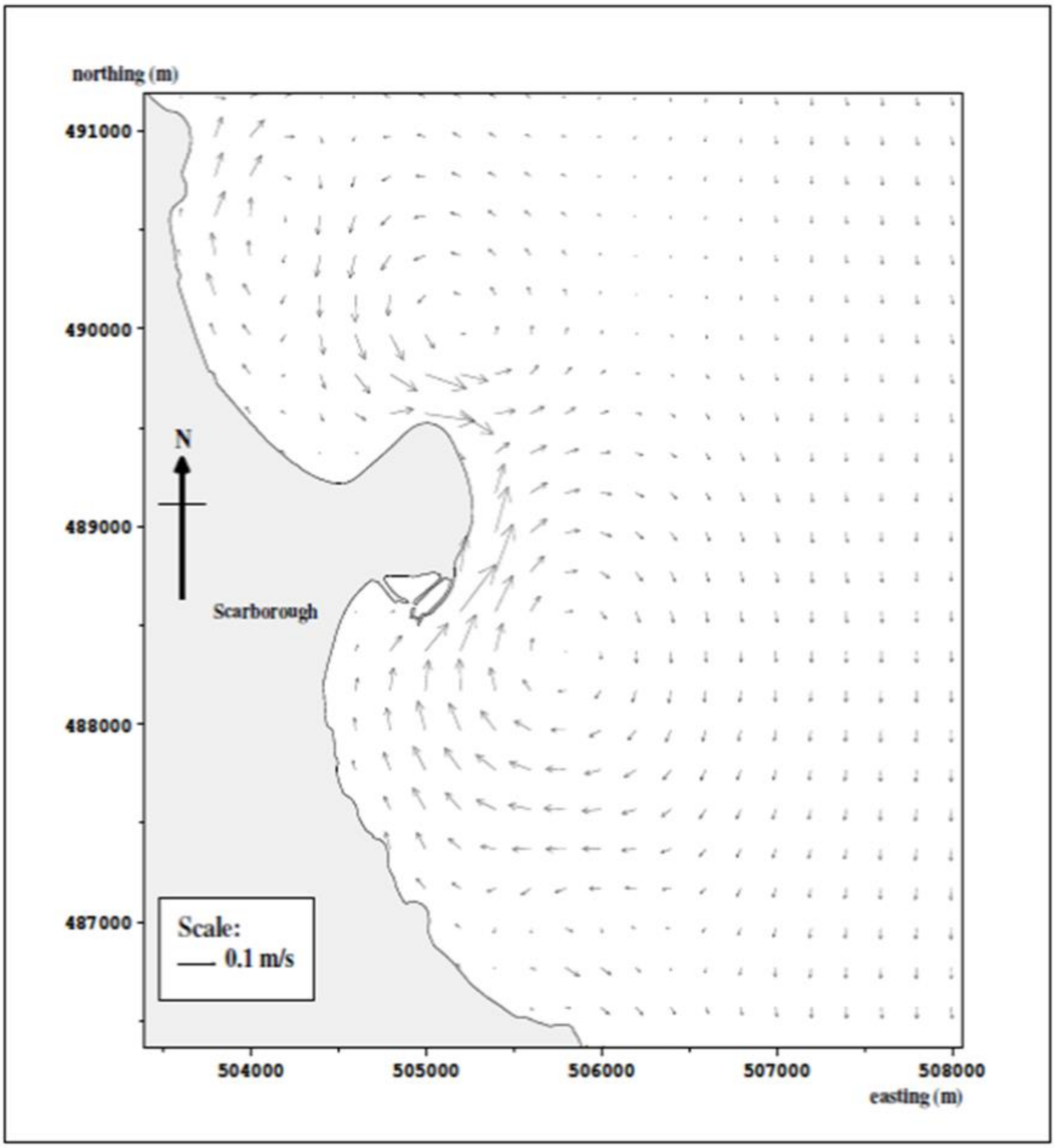

Figure 1. postulated tidal current pathways in the nearshore region of Scarborough South Bay

1.2 Study Aims

The aims of the study are two-fold:

1) to test the postulated sediment transport pathways in Scarborough South Bay utilising a particle tracking methodology; and,
2) to test the utility and viability of particle tracking as a valid method for future experiments of a similar nature.

to address the above aims Partrac employed their unique dual signature tracer material and methodology to investigate / track the movement of beach sand, in relation to the above described scenarios (Section 1.1), although no direction was given by the Client to address the offshore bar through sampling.

1.3 Dual Signature Tracers

Partrac use proprietary tracers which are called "dual signature tracers"; this means that each particle (grain) of tracer has two signatures which are used to identify the particle unequivocally following introduction into the environment. The use of two signatures is an advancement and improvement on previously used (mono-signature) tracers. The two signatures are fluorescent colour and paramagnetic character. Two types of dual signature tracer are available: coated particles, and entirely artificial particles. Coated particles possess a fixed grain density of ~ 2500 - 2600 kg m^{-3} whereas that for artificial particles can be adjusted through the range 1010 to 3750 kg m^{-3}. Coated particle grain sizes range from ~20 µm to 5 mm; artificial particles are commonly used to mimic low settling velocity particulates, such as biological larvae, and for engineering scale model studies. Whilst compositional data for each tracer type is commercially confidential, coated particles (used most frequently in tracking studies) are made from natural materials plus a geochemically inert fluorescent pigment. A coated particle is used this this study.

Four spectrally distinct fluorescent colours are available with which to label tracer. These are commercially available fluorescent pigments, which themselves comprise polymer nanospheres embedded with a water insoluble dye. Each pigment is characterized by specific excitation and emission wavelengths, which facilitates a targeted sample analysis procedure, but all are consistently reactive upon exposure to ultraviolet light. Use of multiple colours means that the technology can be used to label multiple sources in the same general area, or to perform consecutive studies in the same area under differing hydrodynamic conditions (e.g. high discharge, low discharge).

Every tracer particle is also para-magnetic. Para-magnetic minerals are not magnetically attracted to one another ('magnetic flocculation') but the para-magnetism gives each particle a magnetic attribute which means that particles will adhere to any permanent or electro-magnet if they come in close proximity. This facilities a simple separation of tracer within environmental (water, sediment, soil) samples, a process which can also be exploited *in situ* (e.g. through use of submerged magnets in a water course; e.g. Guymer, *et al.*, 2010). The integration of tiny magnetic inclusions onto the kernel particle during tracer manufacture is a substantial innovation over mono-signature, fluorescent-only tracers, for which there was no effective means of tracer separation within samples prior to analysis. This has profoundly limited tracer enumeration in many previous studies.

The 'degree of para-magnetism' of a granular material i.e. how magnetic grains are in comparison to quartz-rich beach sand, can be determined quantitatively through use of a magnetic susceptibility sensor. This essentially measures the disruption to an applied low frequency, low intensity alternating magnetic field; ferrous materials naturally possess a greater propensity to disrupt a magnetic field in comparison to all naturally occurring non-magnetic minerals and hence they can be detected using this technique. Typically manufactured tracer is ~400-500 times 'more magnetic' than quartz-rich beach sand. The para-magnetic attribute of tracer can also be exploited in situ through use of a field-portable, hand-held magnetic susceptibility sensor, which can be used in a semi-quantitative fashion to map tracer concentration on soil or sediment surfaces (van der Post, 1995; Black *et al*., 2007).

2. TRACER DESIGN, MANUFACTURE AND TESTING

2.1 Introduction

A site visit was undertaken at the outset of the project to meet with the Client (7th April, 2014), during which we collected 18 surface beach samples which are required for tracer design and beach baseline characterisation purposes. These samples were analysed for the following parameters:

- particle size distribution;
- sediment (sand) density (specific gravity),
- para-magnetic character and
- fluorescent properties.

2.2 Beach Sand Sedimentology

Table 1 summarises the grain size data, which show a range in grains sizes from 138 μm (d_{10}) up to 413 μm (d_{90}) and a slight fining on the lower shore region. This classifies the beach material as 'fine to medium sand' from a hydraulic perspective.

Sediment density (specific gravity) measurements were performed on collected beach material samples using a standard volumetric methodology (BS 1377: 1990 Part 2: 8.2). The density established for material was 2709 kg m^{-3} @ 20^{0}C ± 115 kg m^{-3}.

Table 1: Summary particle size data for beach material samples collected from various locations. LB=lower beach; MB=mid-beach; HB=high beach.

Sample	d_{10} (μm)	d_{50} (μm)	d_{90} (μm)
SBLB	136	219	344
SBLB	138	220	344
SBLB	144	226	351
SBLB	137	215	333
SBLB	136	214	331
SBLB	139	217	335
SBMB	153	258	413
SBMB	155	259	413
SBMB	157	259	413
SBMB	150	245	383
SBMB	152	245	382
SBMB	156	249	387
SBHB	147	254	393
SBHB	151	255	392
SBHB	154	258	402
SBHB	133	255	398
SBHB	137	255	398
SBHB	145	257	398

Direct illumination of beach sand using a blue light showed that there was not any fluorescent character associated with the native sand. However, as is commonly found on many UK beaches, there is a minor magnetic fraction admixed within the principal, quartzitic non-magnetic sand matrix. The presence of this material constitutes 'noise' in terms of using a magnetic tracer to assess sand transport pathways and must, as a consequence, be quantified.

In order to measure the mass ratio of this fraction, 3 beach samples were spread evenly on a white tray. A powerful (11,000 gauss) permanent magnet was then swept across the sample at a distance of 4-5 mm, which removed any magnetic particles. The sample was swept repeatedly until no further material was collected by the magnet and no change in mass was observed. Table 2 presents the results from this analysis showing a mass fraction of natural magnetic particles of 0.17 – 1.16 %, average = 0.73%.

Table 2: Summary magnetic fraction of the native sediment.

Sample	Native sediment mass (g)	Magnetic material (g)	Percentage magnetic material (%)
1	9.96	0.09	0.904
2	5.79	0.01	0.173
3	13.44	0.15	1.116

2.3 Tracer Design and Hydraulic Characterisation

750 kg of fluorescent (green), enhanced para-magnetic tracer sand was manufactured using the foregoing design data. This material was tested for its sedimentological and hydraulic character (grain size, density, fluorescent and magnetic attributes) as part of the hydraulic matching process; this is a process undertaken to demonstrate the hydraulic similarity of the tracer material to the native beach sand. One of the chief assumptions within sediment tracking studies (Foster, 2000) is that the tracer's hydraulic and bio-organic properties mimic those of the sediment of interest, and therefore the tracer is transported in the same fashion as the native sediment.

The spectral properties of the green fluorescent dye are covered in this Section 2.3.5.

2.3.1 Grain Size

Size spectrum measurements were made on a small sub-sample of the bulk tracer batch using the *Mastersizer 2000* Laser Diffraction instrument. Figure 2 presents data from this analysis. Respective values of the d_{10}, d_{50} (median) and d_{90} percentiles are 165 μm, 260 μm and 431 μm.

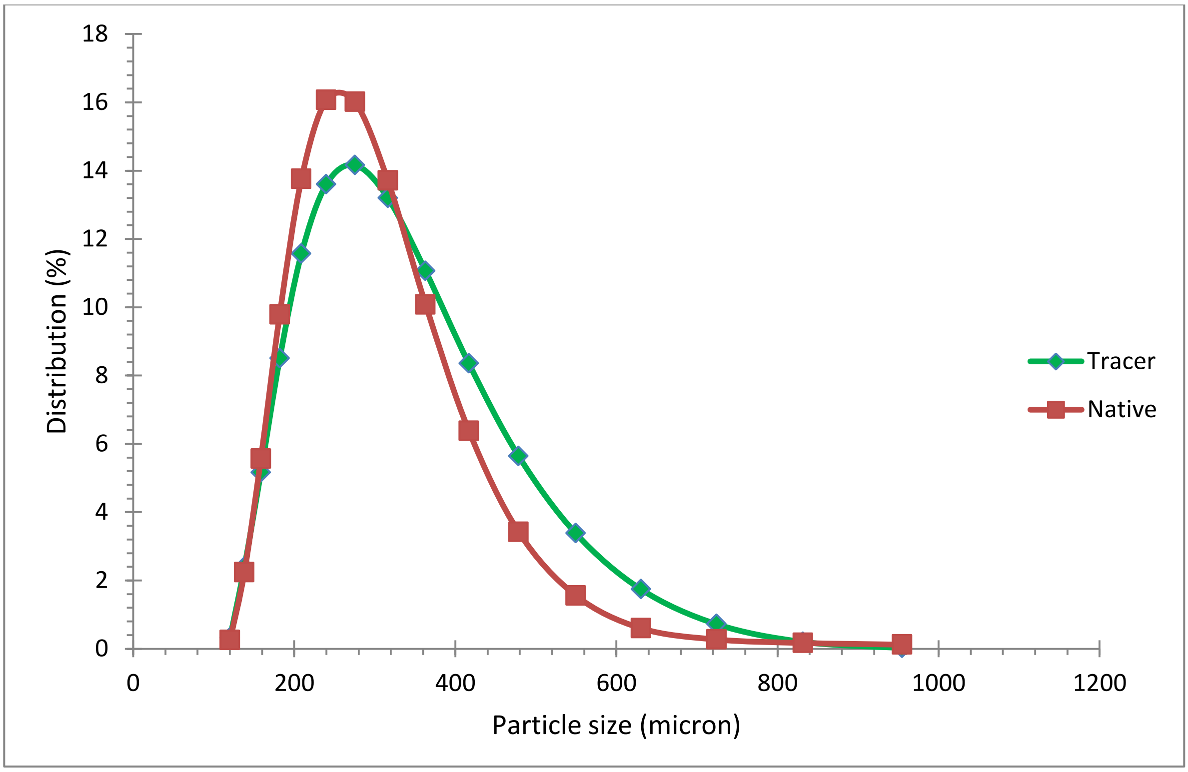

Figure 2. Comparison of the particle size distribution of the manufactured tracer and native beach sediment.

2.3.2 Grain Density

Direct measures of tracer density were made using a standard volumetric methodology (BS 1377: 1990 Part 2: 8.2). This gave a density of 2,436 kg m^{-3} for the tracer (only one sample was analysed).

2.3.3 Para-Magnetic Attribute

Particles with para-magnetic attributes were required, in order that magnets could be used both within field sampling and to achieve magnetic separation (i.e. separation of magnetic particles [including tracer]) from non-magnetic sediments). Para-magnetism can be quantitatively confirmed using a specific laboratory test which measures directly the geological mass-specific magnetic susceptibility (χ) of a tracer. This provides an index of the relative ease of which a soil or sediment sample can acquire magnetic attributes in the presence of an applied, low frequency (100 μT) alternating magnetic field. Ferruginous (i.e. iron rich) materials possess a greater propensity to acquire a magnetic attribute, and therefore display relatively high values for χ, whereas largely non-ferrous materials do not. The low frequency magnetic susceptibility was determined using a Bartington MS2B susceptibility sensor for 3 sub samples of tracer and 3 sub samples of a quartzitic beach sand sourced from Scarborough, South Bay, Yorkshire, UK to provide a comparison between a coated material (tracer) and an uncoated material. The results (Table 3) show that the coated tracer material is ~128 times 'more easily magnetised' than the South Bay beach sand.

Also, a simple test was designed to establish the percentage (%) of particles that are magnetic (Table 4). To do this, a high force bar magnet (~11,000 gauss) was held in suspension just above the sample and carefully passed over the sample three times. The magnetic material recovered was then weighed and compared to the known mass (g) of tracer particles present within the sample. This test was repeated 3 times. The results (Table 4) show that **<u>100% of tracer particles were magnetic</u>**.

Table 3: Low frequency mass specific magnetic susceptibility (χ_{LF}) of the tracer and a quartzitic beach sand provided as a comparison.

Sample (material)	Mass (g)	Air 1	Sample 1	Sample 2	Air 2	*K* corrected	*Mass specific* χ_{LF} (kg m^{-3})
Tracer	1.866	0.3	165.2	165.2	0.3	165.3	308.4
Tracer	1.736	0.3	179.0	179.0	0.3	179.1	310.9
Tracer	2.012	0.3	159.3	159.3	0.2	159.45	320.8
Mean (χ_{LF})							**313.36**
Quartzitic sand	1.49	0.3	2.4	2.3	0.1	2.55	3.8
Quartzitic sand	1.911	0.1	1.9	1.9	0	2.25	4.3
Quartzitic sand	1.753	0.5	3.0	3.0	0.3	3.0	5.26
Mean (χ_{LF})							**4.45**

Table 4: The percentage of tracer particles that are magnetic.

Sample	Tracer mass (g)	Tracer mass recovered (g)	Percentage of tracer particles recovered (%)
1	10.23	10.23	100
2	8.67	8.67	100
3	5.69	5.69	100

2.3.4 Fluorescent Colour

A sub-sample of the tracer colour was inspected under blue light illumination (UV- A ~ 395 nm) using a high power photomicroscope to determine the integrity of the fluorescent-magnetic coating and the quantitative % of coated particles. These tests (Figure 3) indicated **100% of particles are coated**.

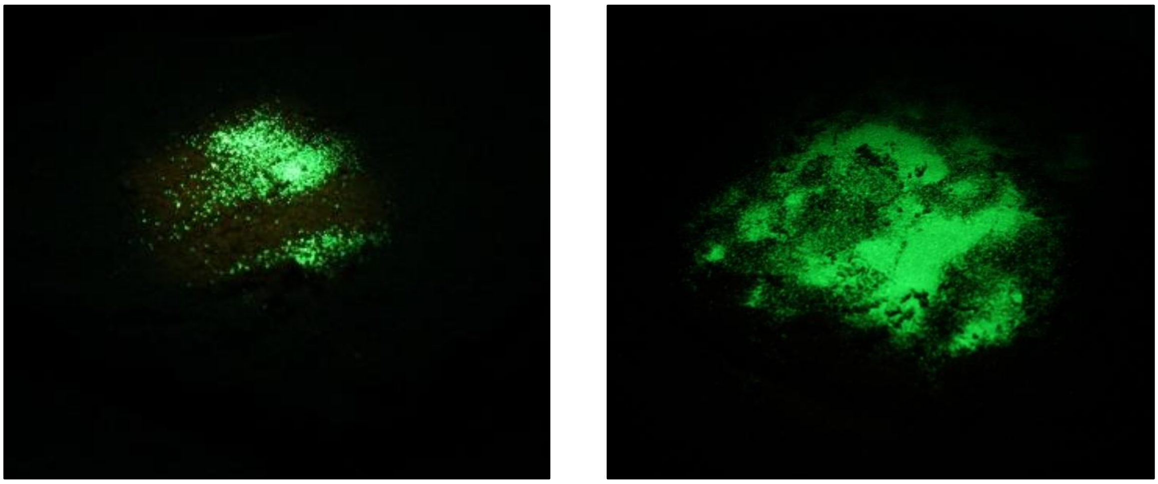

Figure 3. Photograph of the green tracer mixed with native beach sand at a concentration of 0.001 g cm^{-2} (left) and 0.185 g cm^{-2} (right) under blue light illumination (UV-A ~ 395 nm).

2.3.5 Spectral Characteristics

Each tracer colour possesses spectral characteristics which are a function of the dye incorporated onto particle surfaces during the coating process. The analysis of dye concentration during the tracer enumeration procedure relies upon transmission of light of a specific wavelength - which optimally stimulates the dye to fluoresce (this is known as the 'excitation' wavelength, λ_{ex}) – and measurement of the intensity of light emitted specifically at the wavelength at which the dye is known to fluoresce (this is known as the 'emission' wavelength, λ_{em}). If these values are known then the measurement of dye concentration (and hence in this context tracer dry mass, *M*) is also optimised.

Figure 4 shows the excitation and emission spectra of the green tracer. The fluorescence excitation spectrum (dark blue line) is obtained by fixing the fluorescence detector wavelength at 523 nm and then scanning the excitation wavelengths. This provides a fluorescence induction spectrum, which is, in effect, an absorption spectrum of the particles. Inversely, the fluorescence emission spectrum was obtained by fixing the excitation wavelength at 485nm and then scanning the emission wavelengths.

The excitation wavelength for the tracer comprises a broad spectrum band from 250 to ca. 500 nm, with a mode centred on 460 – 490 nm with a peak value at 485 nm, whereas the emission spectrum is much narrower and centred on 530 nm. Wavelengths for green tracer colour used in spectrofluorimetric analysis are given in Table 5.

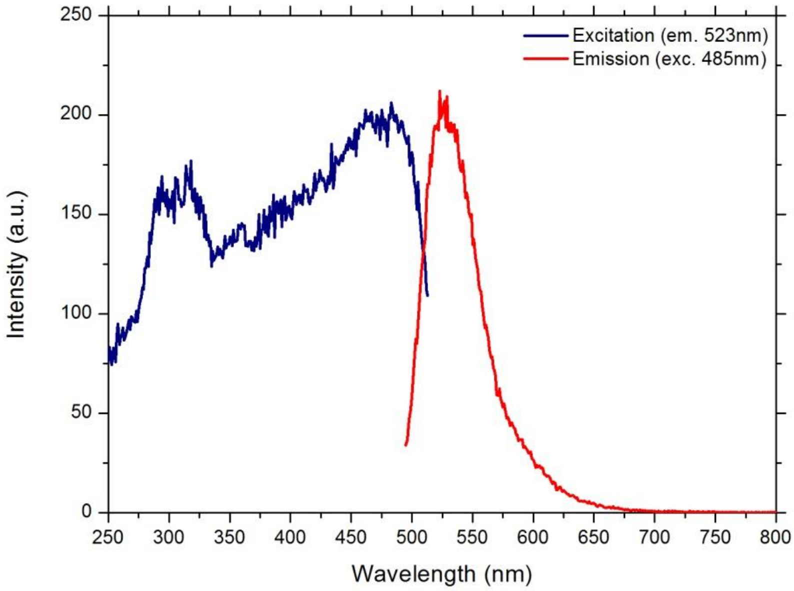

Figure 4. Emission – excitation spectra for the green tracer pigment.

Table 5: Excitation and emission wavelengths for green tracer.

Tracer Colour	Excitation Wavelength λ_{ex} (nm)	Emission Wavelength λ_{ex} (nm)
Green	485	530

2.4 Summary Characteristics

Table 6 provides a summary for each of the native beach sand and the hydraulically matched tracer.

Table 6: Summary of the characteristics of the native beach sand and tracer.

Colour	Quantity (kg)	d_{10} (µm)	d_{50} (µm)	d_{90} (µm)	Particle Density kg m^{-3}	Magnetic Susceptibility χ_{LF} (kg m^{-3})	Magnetic Mass Fraction %	Fluorescent Fraction %
Native Sand		138	242	413	2,709 ± 115	4.45	0.73	0
Green Tracer	750	165	260	431	2,436	313	100	100

3. SURVEY METHODOLOGY

3.1 Introduction

A key consideration for this particular type of study is to judge those marine conditions, in particular the wave climate, which will generate shoreface transport but not 'blow out' the experiment. Initiation of the field study and tracer material injection required a period of relative quiescence in marine conditions to allow tracer introduction/injection. To this end we aimed to prepare the study so that it was 'ready to go', and to use all available information that can predict the marine conditions for the immediate 5 days.

In early December 2014 it was decided that the forecasted conditions appeared favourable for the initiation of the field study and tracer material introduction.

3.2 Tracer Preparation and Introduction

The tracer material was delivered to Scarborough Borough Council and stored in a council depot prior to commencement of the study. To comply with Marine Management Organisation (MMO) licence exemption criteria for tracing studies (i.e. maximum of 250 kg of tracer material to be injected / deposited per day) the 750 kg of tracer material was divided into 3 batches of 250 kg. The 3 batches of 250 kg of tracer material were introduced onto the beach at 3 locations of the upper foreshore over 3 consecutive days; these areas are subsequently referred to as 'deployment zone(s)'; see Figure 9 and Table 7). Deployment Zone 1 was positioned near the centre of the beach between the lifeguard station to the North and the Spa building to the South. Deployment Zone 2 was positioned 20 m to the North of Deployment Zone 1 and Deployment Zone 3 positioned 162 m to the North of Deployment Zone 2.

At each deployment zone location a shallow trench (1 m x 10 m x 4 cm) was dug manually in the upper foreshore. The trench was excavated in 1 m^2 blocks, 50 % of the native sediment removed was mixed with the tracer in a cement mixer with 25 kg of tracer (50/50 ratio), and a small amount of seawater was added (< 5 L). The tracer/native sand admixture was then carefully re-introduced to the trench, raked into position and lightly compacted manually to (as best as possible) match naturally occurring conditions (see Figure 5 and Figure 6). This process was repeated until a 10 m^2 surface coverage area was achieved. Examination of exploratory cores collected after deployment showed a mean tracer bulk density (wet mass / wet volume) within the deployment zones of 1,460 kg m^{-3}.

Figure 5. Deployment of the Tracer Material at Deployment Zone 2

Figure 6. Deployment of the Tracer Material at Deployment Zone 2

Figure 7. Deployment of the Tracer Material at Deployment Zone 3

Figure 8. Deployment of the Tracer Material at Deployment Zone 3

Table 7: Date and location of deployment zones, location fixed from upper foreshore southern edge of zone (SW corner). Coordinates are OSGB National Grid)

Deployment zone	Date of Deployment	Location	
		Easting	Northing
1	3rd December 2014	504433.632	488231.599
2	4th December 2014	504440.765	488253.719
3	5th December 2014	504486.988	488415.419

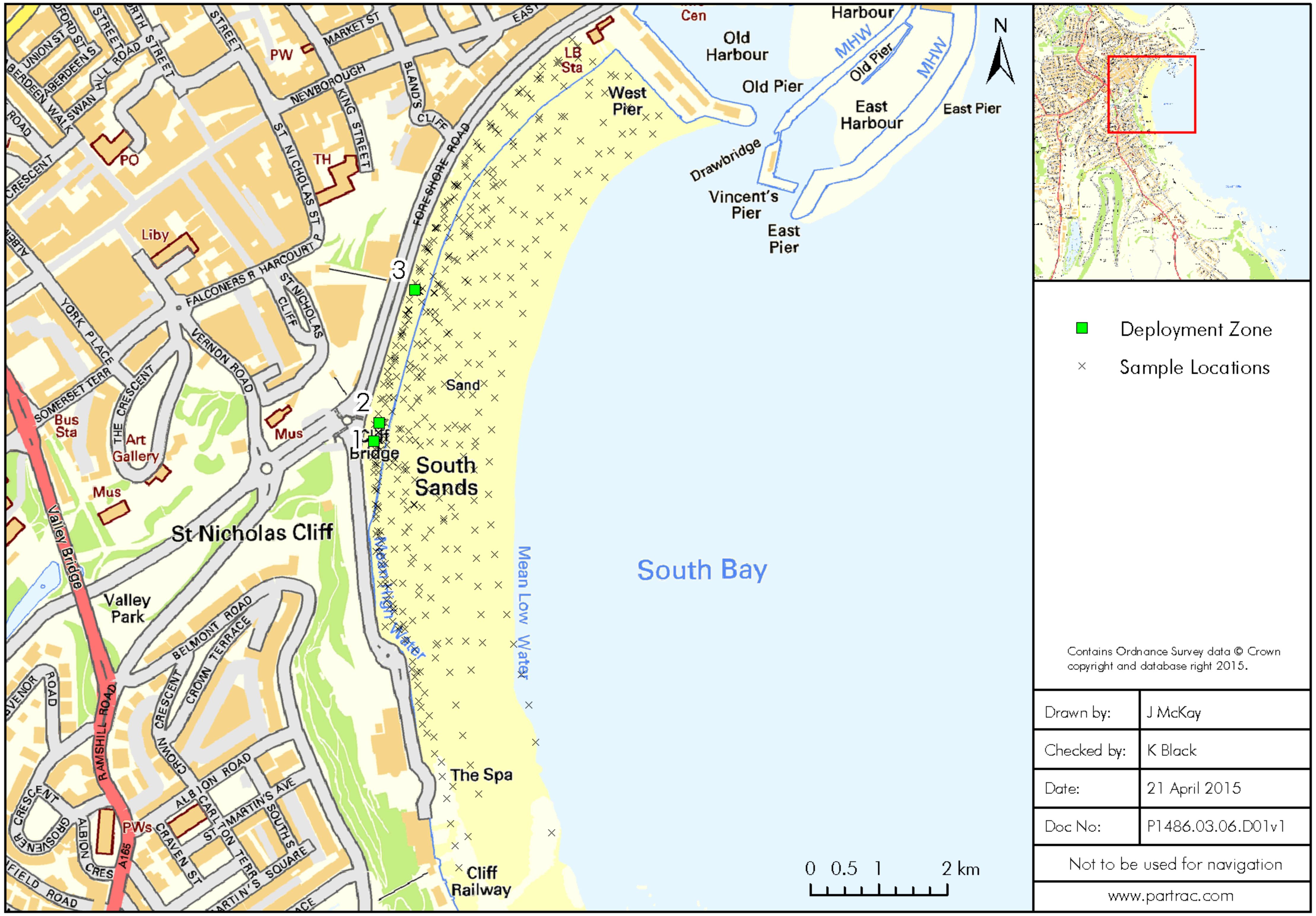

Figure 9. Location of tracer material Deployment Zones and of the entire sample set collected for the six sampling campaigns.

3.3 Navigation & Positioning

Positioning was undertaken using a Trimble R4 GNSS RTK base and rover system operated using a Trimble TS32 controller. Using this survey system enabled the position of each deployment zone and sample collected to be determined with cm precision accuracy. A Garmin handheld GPS system was used when the rover and base system was unavailable.

Figure 10. Trimble R4 GNSS RTK base and rover system used for positioning during the study.

3.4 Sampling

This study utilised both qualitative and quantitative experimental data to rigorously reveal the transport pathway and depositional footprint of the tracer particles. A multi stage sampling campaign was conducted over a 54 day period involving the collection of shallow sediment surface samples, extensive visual survey (night-time blue lamp survey) and low frequency magnetic susceptibility measurements. In particular, the blue lamp survey was useful in delineating beach face areas suitable for the collection of surface sand samples.

3.4.1 Surface samples

An exploratory trench cut into each deployment zone prior to the collection of sediment surface samples provided a vertical concentration profile. Within that profile the tracer provides a horizon marker that can be used to estimate the depth of material in transit, termed 'the active sediment layer' (King, 1951, Inman and Chamberlain, 1959, Komar, 1969). This was determined as 4-5 cm. Sampling of the beach face must incorporate the active sediment layer, and for this reason samples were collected to a depth of 6 cm. To collect a sample a survey quadrat (0.01 m^2) was placed on the sediment surface and manually excavated using a trowel. Sampling campaigns were conducted 1, 2, 3, 7, 14 and 54 days after the first wave event. The 6 sampling campaigns resulted in the collection and analysis of 493 samples. Figure 9 shows the locations of all of the samples collected for the 6 sampling campaigns

3.4.2 Night-time fluorescence

The spectral characteristics of the tracer enable unequivocal identification of the tracer particles within the environment using a blue light torch (emitting wavelength 395 nm). Using these torches transects of the beach were walked at during darkness (night) at low tide by pairs of survey staff to visually assess the spatial distribution of tracer particles on the beach surface prior to and following high energy wave events. Night time survey transects were undertaken after each tidal inundation following the deployment of tracer to each deployment zone and at the end of the spring – neap tidal cycle, resulting in 4 night time surveys being conducted. A 'sampling diary' was kept by the survey staff involved, and a qualitative description of the spatial distribution of tracer particles was recorded following each night time survey. This was particularly useful in determining the spatial distribution of the tracer particles following inundation, prior to the first wave event.

3.4.3 Magnetic susceptibility (χ)

Mass-based magnetic susceptibility is a comparative measure of the relative ease with which a material can acquire a magnetic field when exposed to a low frequency (100 μT) alternating magnetic field. Ferrous or iron-rich particles acquire a magnetic field far more easily that non-ferrous particles. Low frequency magnetic susceptibility measurements were made using a Bartington MS2 magnetic susceptibility meter connected to an MS2D surface scanning probe operated in conjunction with the MS2 probe handle. This loop probe provides rapid assessment of the magnetic content (SI) of magnetic materials in the top 100 mm (50 % at 15 mm, 10 % at 60 mm) of the land surface and in this context was used to measure tracer depletion from source (deployment zones). To do this, the magnetic susceptibility of the native sediment within each deployment zone was measured prior to and following tracer introduction then re-measured following the initial wave event.

3.5 Supporting Oceanographic Data

Coastal wave data were retrospectively obtained from the CCO Regional Coastal Monitoring Wave Buoy Network (Scarborough Buoy), located 54 17.598'N 0° 19.077'W, for the period of the study (from 5th December to 19th December, 2014).

4. TRACER ENUMERATION

4.1 Introduction

Spectrofluorimetry was the method employed to determine the dry mass of tracer (in grammes) within a sample. A fluorimeter is a device used to measure parameters of fluorescence: its intensity and wavelength distribution of emission spectrum after excitation by a certain spectrum of light. These parameters can be used to identify the presence and the amount of specific dye molecules in a fluid medium. Modern fluorimeter's are capable of detecting fluorescent molecule concentrations as low as 1 part per trillion. This approach offers a means with which to obviate the additional mass due to the presence of magnetic but non-fluorescent particulates[1] simply and directly. It also provided a very high analytic resolution which would facilitate detection of very low (mg quantities) tracer mass. The fluorimeter signal output can be empirically related to tracer mass (kg or g) through a series of tracer (colour) specific, reference standards.

Prior to use of the spectrofluorimetric method environmental samples are pre-processed. The chief aim of pre-processing is to remove all native non-fluorescent, non-magnetic particles.

4.2 Sample Preparation

Each sample is dried in an oven at 80°C until no further change in mass is observed. The magnetic and non-magnetic fractions are usually separated using a Franz Vertical Isodynamic Separator[2]. This is a device used in commercial mining to separate out magnetic residues in granular substances. In this project, however, the large number of samples and analysis timeframes using this approach was preclusive. Thus an alternative approach was developed.

Following drying each sample is smoothed to an approximately granular monolayer on a large white board; the sample is then inspected visually for tracer particles. A permanent Ne-Bn 11,000 Gauss magnet is then scanned across the sample at a distance of 2-3 mm, facilitating separation of magnetic particles. This procedure is repeated, with intermittent cleaning and recovery of the particles from the surface of the magnet, until no further magnetic particles is extracted.

The magnetic fraction is then ready for fluorimetric analysis.

4.3 Gilden Photonics™ Fluorimeters

The analyses were carried out using a Gilden Photonics Fluorosens fluorimeter. The Fluorosens fluorimeter incorporates single photon counting sensitivity into a fully computer controlled spectrometer (Figure 11). As the peak excitation and emission wavelengths of the dye coating is known (peak excitation 485 nm, peak emission 523 nm) an emission scan across the emission wavelengths (500 – 600 nm) provides fluorescent intensity (V) readings at the chosen emission wavelength (530 nm). Each sample was run in triplicate and the mean value determined.

Figure 11. The Fluorosens laboratory fluorimeter.

The Fluorosens fluorimeter is especially suited to the present task as measurement is recorded in a highly stable controlled environment. The general technical specification of the Fluorosens instrument is provided in Appendix I.

4.4 Methodology

A detailed **Standard Operating Procedure** for the analysis is commercially sensitive information. The method in general terms involves a series of common steps:

1. drying and weighing of the sample (sieving if necessary);

2. dissolution of the fluorescent pigment into a special solvent for a period of 168 hours (7 days);
3. centrifugation if necessary (to remove all particulates);
4. dilution to a known level using analytical grade solvent;
5. analysis of the fluorescence intensity of the dye solution using a Fluorsens fluorimeter; and then
6. derivation of tracer particle dry mass (M_g) using calibration functions (dose response curves).

4.4.1 Standard (Dose Response) Curves

Eluted dye solutions for the green tracer are prepared by adding a known dry mass of tracer particles to a known volume of analytical grade solvent. The solution is then left to equilibrate for 168 hours (7 days). This time period has been established as optimal for maximal extraction of the pigment into the solvent. Dose response curves were obtained by filling the calibration cell with 3 ml of analytical grade solvent, recording a baseline reading and then adding sequential 20 μl aliquots of the stock solution, mixing and recording further readings.

If there is a sediment fraction in collected samples which is non-fluorescent but magnetic (i.e. therefore recovered with the magnet method used; this is the case on Scarborough beach), it can affect the intensity of emitted radiation received by the sensor (termed 'quenching') during fluorimetric analysis. Thus, dose response curves were prepared with both tracer and native beach material to account for the quenching effects of the native material. Consequently 4 individually tailored dose response curves were prepared to enumerate the tracer mass from the samples collected, 2 dose response curves representing samples of high sediment load and 2 representing samples of low sediment load for samples collected using *in situ* magnets and grabs respectively. Dose response curves were prepared as follows:

1. Low sediment volume - 0.01g tracer; 1.5 g background native material (average background material concentration following magnetic separation), sequential readings through to 0.1g; and
2. Intermediate sediment volume – 0.1 g tracer; 3 g background native material (average background material concentration following magnetic separation), sequential readings through to 1 g; and
3. High sediment volume – 1.5 g tracer, 15 g background native material (average background material concentration following magnetic separation), sequential readings through to 15 g

Least-squares regression analysis (Fowler *et al*., 1998) was performed on the data to generate calibration functions.

4.4.2 Tracer Enumeration

To determine the dry mass (*M*, g) of tracer in a in a sample containing 1 tracer colour, the respective regression equation is used to determine dye concentration from probe response. To derive dye concentration the regression equation must be inverted to enable determination of dye concentration (DC) from the fluorimeter signal. Tracer dry mass (TDM) is then calculated using the following equation;

$$TDM = \left(\frac{DC}{DC_{max}}\right) \times TDM_{max} \qquad 1.$$

Where, DC_{max} is the maximum assumed dye concentration (ug L^{-1}) and TDM_{max} is the equivalent tracer dry mass value.

4.4.3 Quality Assurance

An analytical quality control/assurance methodology was developed in tandem with development with the fluorimetric method. This involved inclusion of the following within the laboratory testing strategy:

1. Periodic testing of blanks
    a. 15 blanks tested;
2. Periodic testing of blind samples (i.e. tracer masses unknown to the technician);
    a. 3 samples tested.

4.4.4 Visual Observations

Prior to fluorimetric analysis all samples were routinely visually inspected under UV illumination to assess tracer presence. Qualitative descriptions, which are given a number from 1 to 5, were developed as follows:

1. Trace = ~< 0.005g
2. Low = ~< 10^{-2}g
3. Intermediate = ~< 10^{-1}g

4. High = ~< 0.5g
5. Very high = ~10^0g

Note:- Due to quenching effects[3] of the background non-fluorescent, magnetic material and the low wavelength of a standard UV-A inspection lamp (~400nm), and since not all the sample is examined in depth, the probability exists *of a negative visual inspection and a positive fluorimetric result*. Cross-comparison of qualitative descriptions with fluorimetric data should accordingly be undertaken with caution.

3 Quenching is any process that decreases the fluorescent intensity of a sample (Lakowicz, 2006).

5. CALIBRATION AND QUALITY CONTROL

5.1 Dose Response Curves

Standard (dose response) curves were developed to relate fluorimetric measurements (probe reading in volts) to tracer dye concentration over the range of dry masses (0.01 – 0.1 g, 0.1 - 1 g and 1.5 – 15 g) (Figure 12). Consistently high coefficients of determination (r^2) are found (Table 8).

Table 8 Summary of r^2 values of the dose response curves for differing background sediment loadings.

Sample Type	Sediment Load	r^2
Beach face	Low	0.99
Beach face	Intermediate	0.98
Beach face	High	0.99

5.2 Minimum Resolvable Mass (MRM)

The MRM is derived from the lowest possible fluorimeter response (which is 1 volt). This value is then propagated through the regression equations of each dose response curve to determine the MRM, which is given by the intercept of the regression line on the y-axis. MRM values are summarized in Table 9 for high, intermediate and low background sediment loads.

Table 9 Summary of MRM values for each dose response curve.

Sample type	Sediment Load	MRM (g)
Beach face	Low	0.008
Beach face	Intermediate	0.063
Beach face	High	0.034

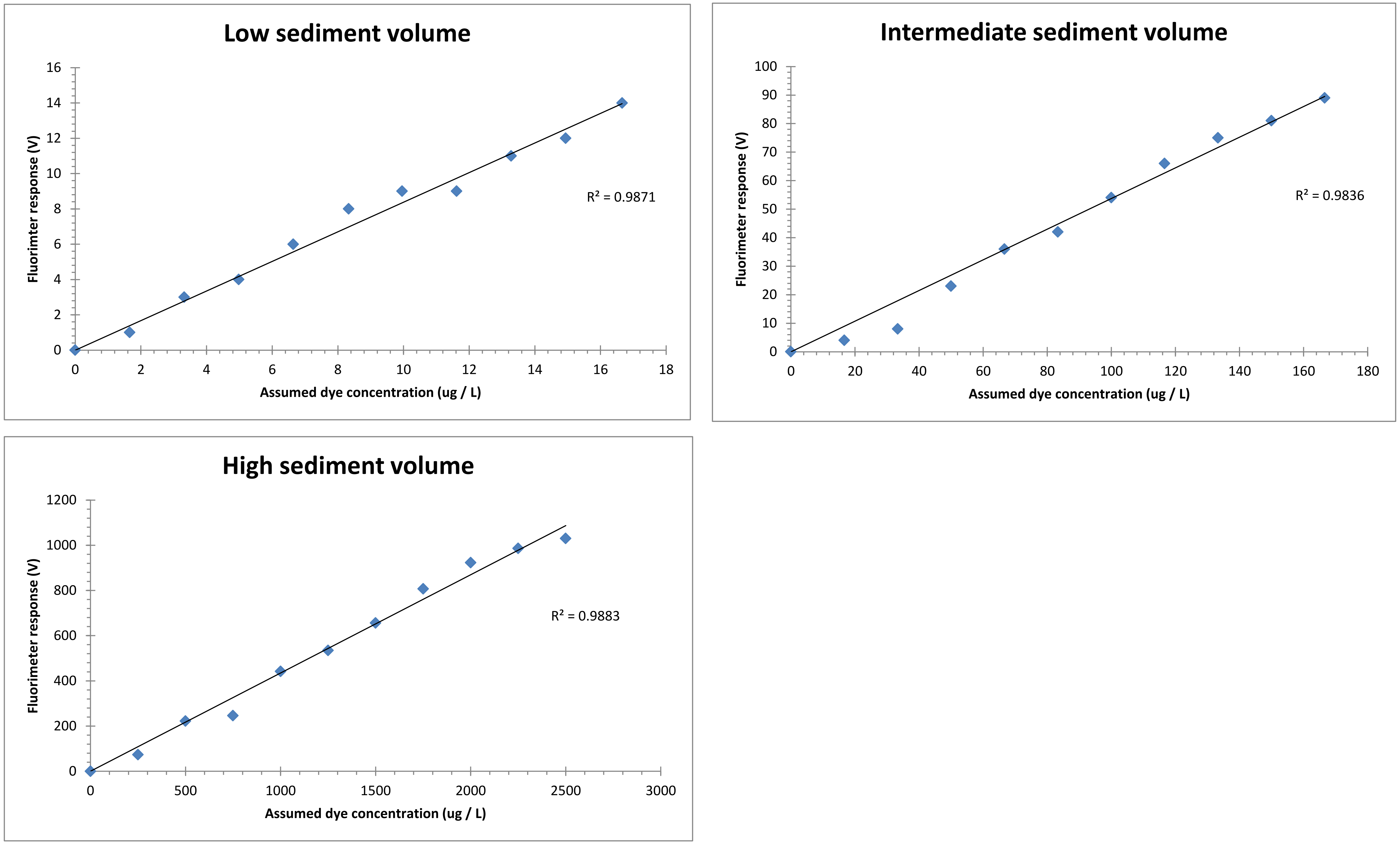

Figure 12. Dose response curves for Low, Intermediate and High sediment volume for all the samples collected. In practise the point concentration values on the x-axis are interchangeable with the corresponding tracer dry mass of each curve.

5.3 QC Data – Periodic Testing of Blanks

A check on the performance of the fluorimetric analytical procedure is made through periodic testing of blanks (Table 10). Blanks are solutions made up in entirely the same manner as samples but without inclusion of a sediment/tracer sample.

Table 10: **Periodic testing of laboratory blanks for mono-colour (green) tracer dye.**

Sample #	Blank Tracer Mass M_{blank} (g)
1	0.000
2	0.000
3	0.000
4	0.000
5	0.000
6	0.000
7	0.000
8	0.000
9	0.000
10	0.000
11	0.000
12	0.000
13	0.000
14	0.000
15	0.000

5.4 Testing of Blind Samples

In order to establish the fluorimetric analytical procedure together with operator efficiency function as desired, periodic blind samples were submitted for testing to the laboratory. Blind samples are prefabricated mono-colour sediment samples within which the tracer dry mass is unknown to the analyst. Table 11 summarises results from testing of three samples. The results are good (within 5% of true value) in terms of analytical accuracy.

Table 11: Periodic testing of blind samples (green tracer).

Sample #	Native sediment mass (g)	Doped Tracer Mass M_{dop} (g)	Measured Tracer Mass M (g)	Mean Error (%)
1	2.86	0.231	0.248	1.8
2	2.98	0.24	0.289	4.6
3	2.09	0.2	0.186	1.9

6. RESULTS AND DISCUSSION

6.1 Tracer Dry Mass Data

Appendix II presents results for all samples tested for tracer dry mass expressed as an area density metric (g m^{-2}). Background samples (i.e. collected before any tracer was deployed), and samples of the beach immediately following tracer introduction, are found at the top of the table. Qualitative visual descriptions (inspection under blue light) are given for every sample (note the general use of caution in Section 6.3.3 if cross-referencing these to fluorimetric data is undertaken).

6.1.1 Quality Control

35 samples were not analysed for tracer dry mass due to sample corruption, and these are clearly annotated in the data table.

6.1.2 Geospatial Presentation of Tracer Dry Mass

Figures 7 through 12 present the results of the sample analysis and the figures reveal aspects of the redistribution of tracer by tidal inundation / wave action through time.

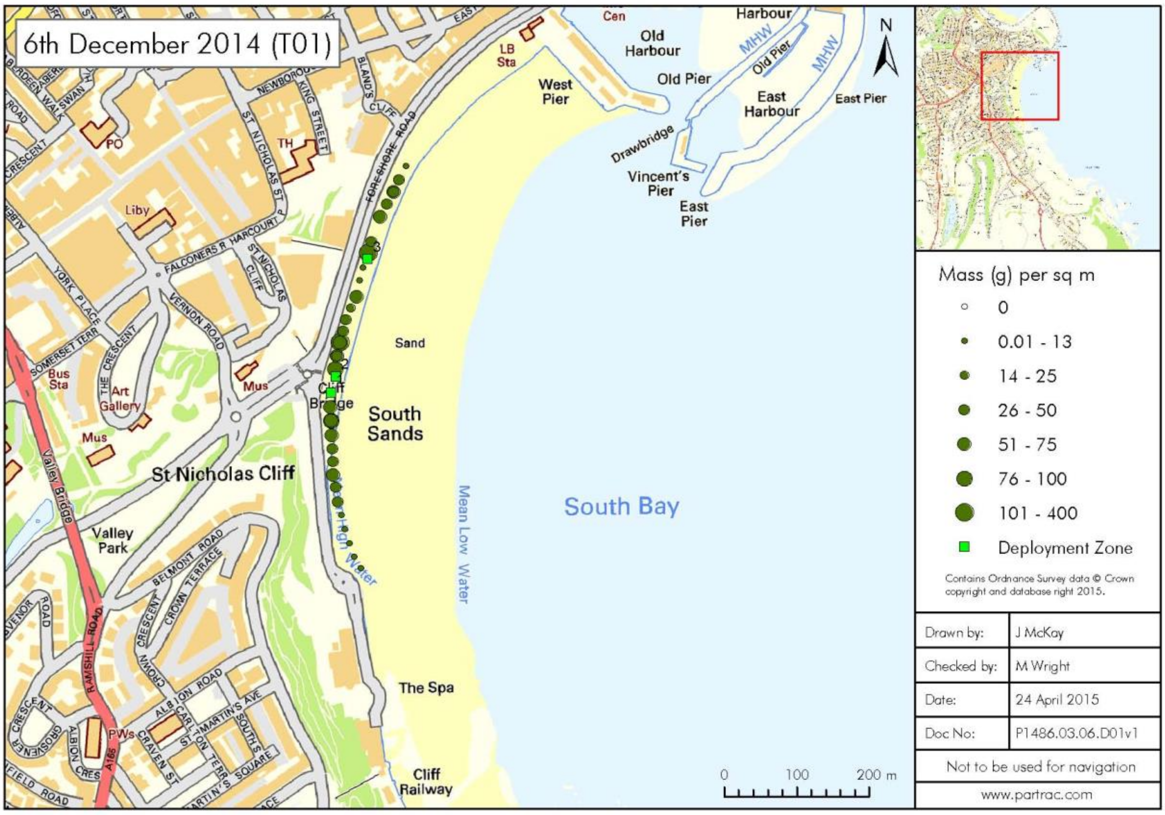

Figure 13. Geospatial distribution of tracer dry mass (g m^{-2}) ~24 hours after injection.

6th December (+36 hours after deployment)

- Inundated 3 times since deployment
- Predominantly Northerly swell direction (from 350° - 20°)
- Sampling undertaken late at night; use of UV torches; sampled only the upper foreshore due to working at night and health and safety implications of this.

Tracer material has clearly moved alongshore from deployment zones in both northerly (~150 m) and southerly (~200 m) directions.

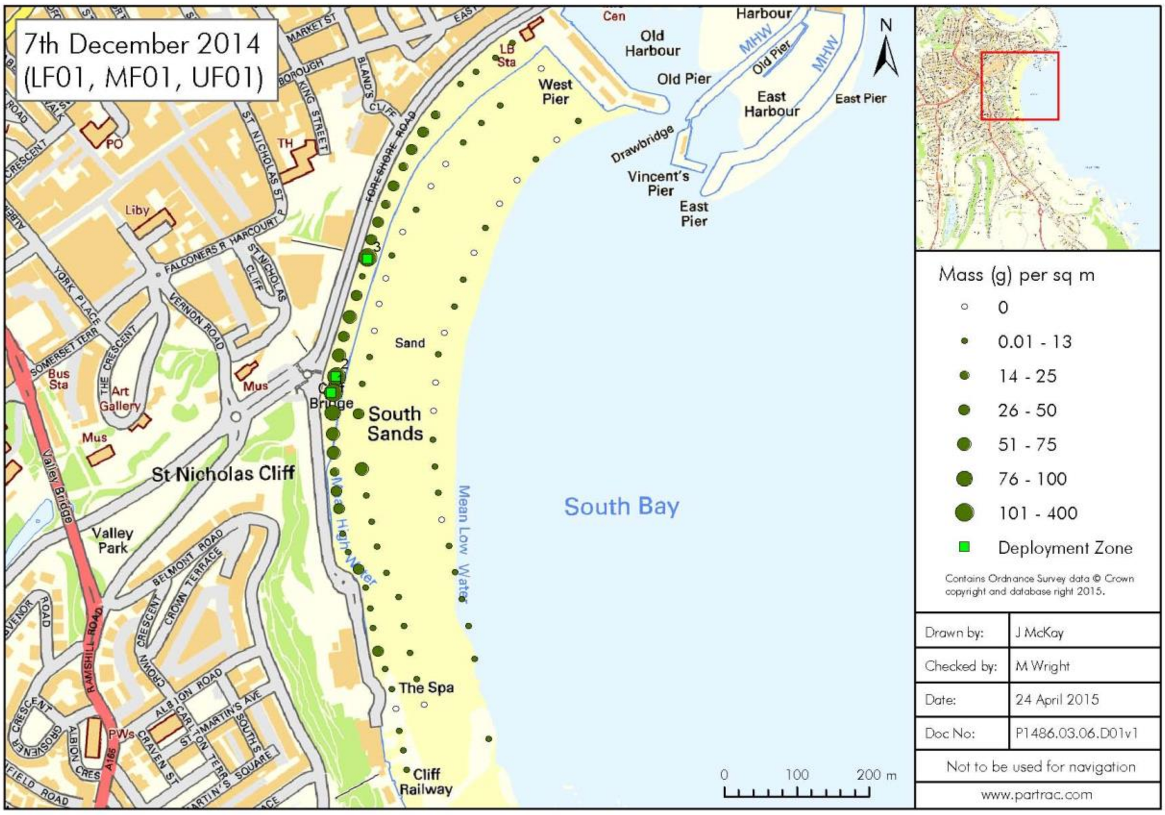

Figure 14. Geospatial distribution of tracer dry mass (g m^{-2}) ~48 hours after injection.

7th December (+48 hours after deployment)

- Inundated 4 times since deployment
- Swell southerly/southeasterly moving to northerly (offshore wave height 0.44 - 0.74 m).

Tracer material has moved both North and South by >250 metres from deployment zones predominantly along the upper foreshore with some cross shore movement

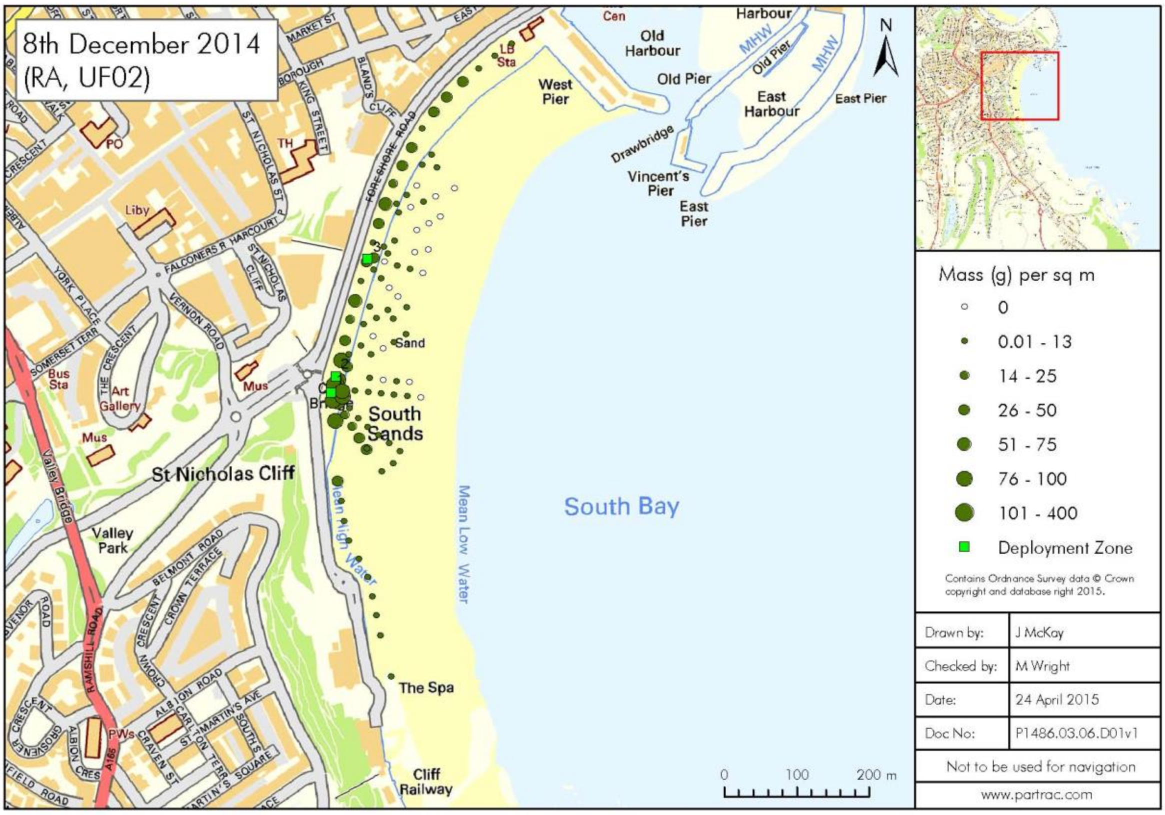

Figure 15. Geospatial distribution of tracer dry mass (g m^{-2}) ~72 hours after injection.

8th December (+72 hours after deployment)

- Inundated 6 times since deployment
- Swell northwesterly to northeasterly (offshore wave heights 0.36 – 1.33 m).

Tracer material has moved in northerly and southerly directions >350 metres from deployment zones with some cross shore movement. Concentrations of material indicate a net northward movement of material in the upper foreshore.

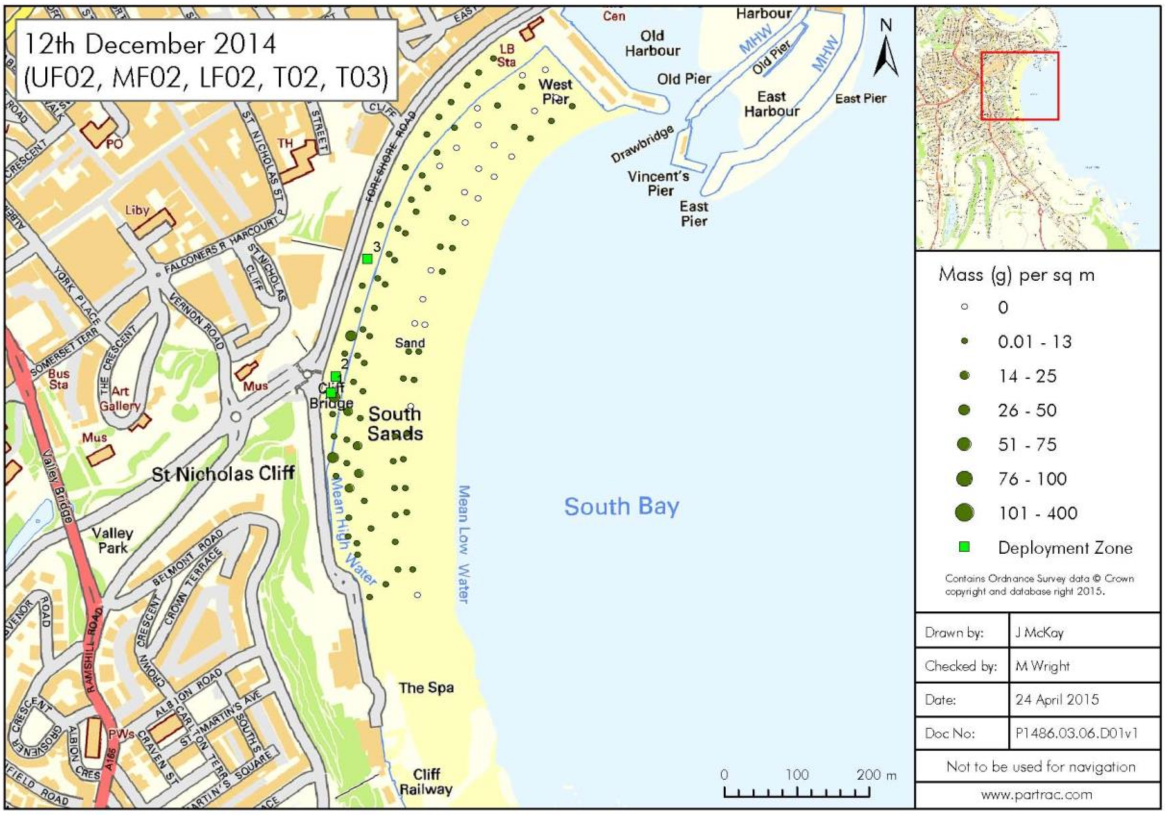

Figure 16. Geospatial distribution of tracer dry mass (g m^{-2}) ~7 days after injection.

12th December (+7 days after deployment)

- Predominantly northerly swell direction (offshore wave heights 0.58 – 2.43 m).

Tracer material has moved in northerly and southerly directions >500 metres. Tracer material is present along much of the upper foreshore north and south of the deployment zones. Cross shore transport of the material has occurred [to some extent] south of the most southerly deployment zone and also seaward of the other two deployment zones. To the northern end of the beach, near the lifeboat station, tracer material is also present in the middle and lower foreshore.

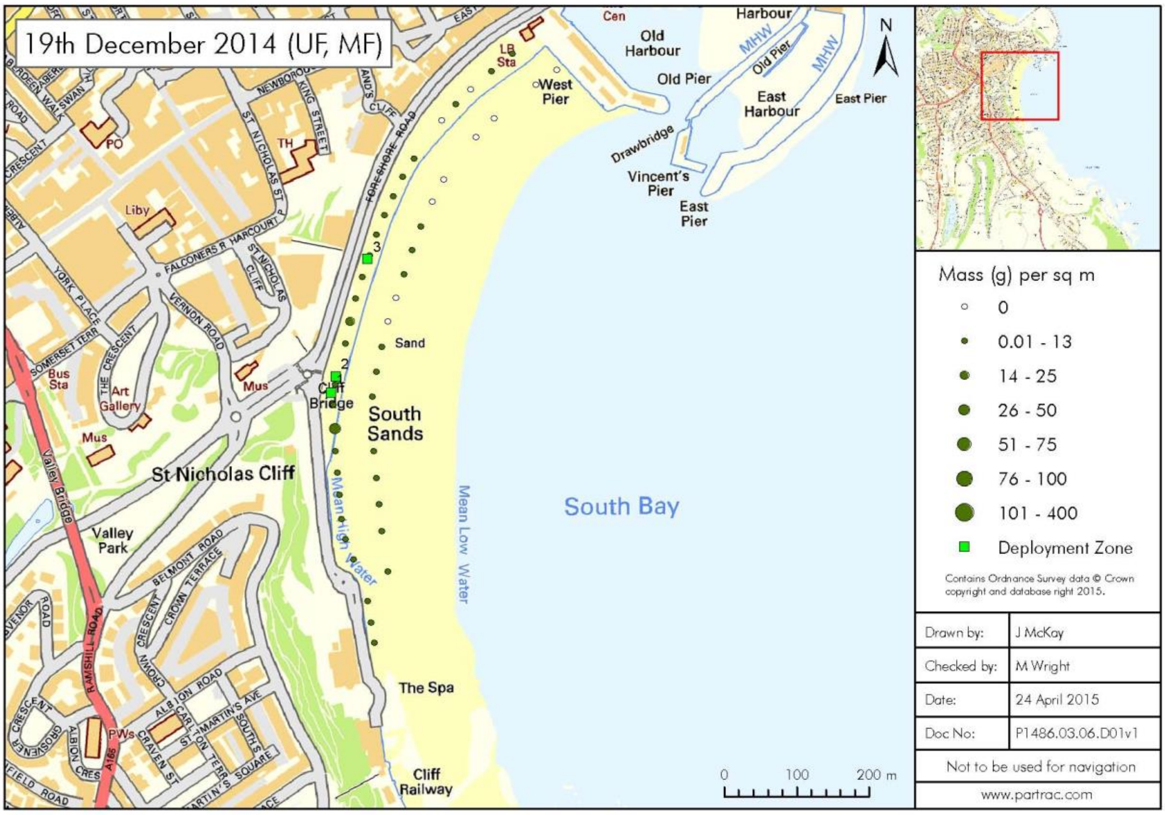

Figure 17. Geospatial distribution of tracer dry mass (g m^{-2}) ~14 days (semi-lunar cycle) after injection.

19th December (+14 days after deployment)

- Predominantly northerly - northeasterly swell direction (offshore wave heights 0.58 – 2.43 m).
- Tracer concentrations low and uniformly distributed along and across the foreshore.

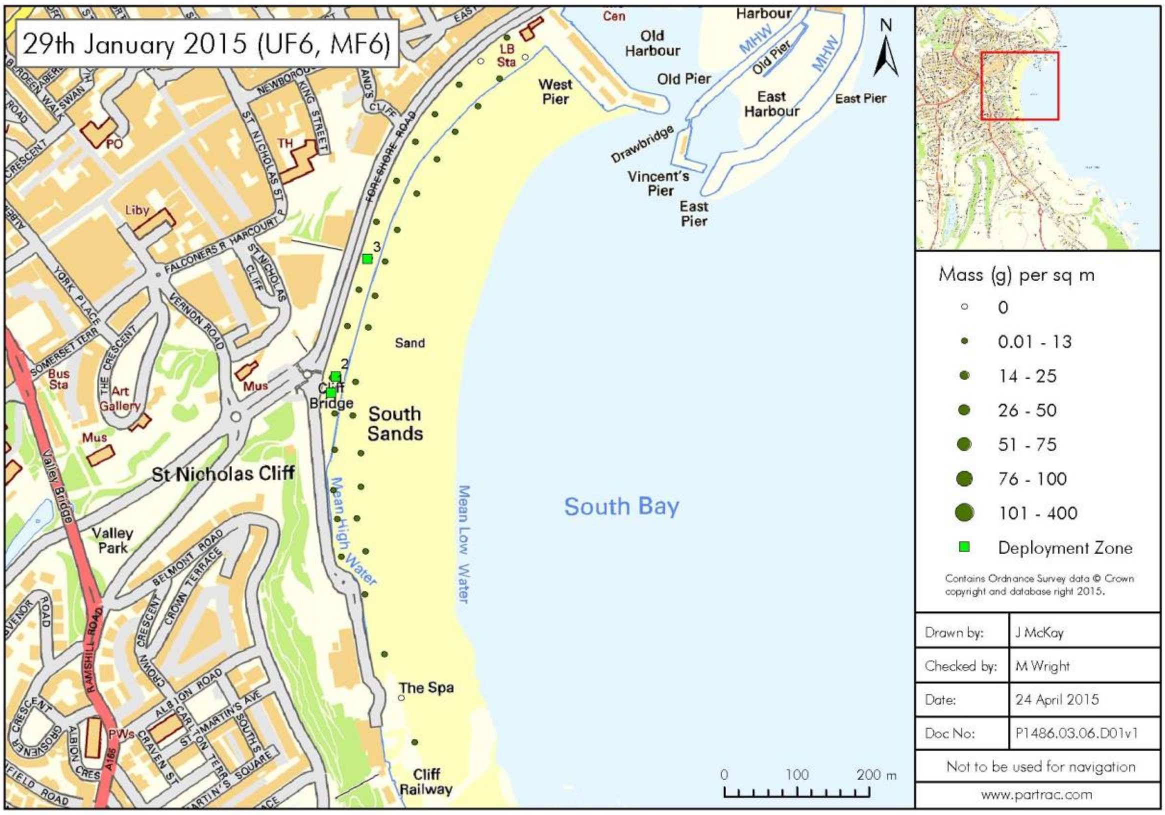

Figure 18. Geospatial distribution of tracer dry mass (g m^{-2}) 54 days after injection.

29th January (+54 days after deployment)

- Predominantly northerly - northeasterly swell direction (offshore wave heights 0.58 – 2.43 m).
- Tracer concentrations low and distributed along and across the foreshore.

As stated previously key to conducting any sediment tracking study is that the results observed only relate to the marine environmental conditions that prevail during the study duration. Table 12 summarises the wave climate through the dominant portion of the study (i.e. to 19th December, 2014), by which point the data indicate a widespread distribution of tracer across the beach-face. As indicated by the wave data within the study duration the study site received waves from all directions bar due East, and therefore the tracer results in this sense fundamentally reflect a mixed wave climatology.

An additional consideration is to perform a study which isn't 'blown out' by overly energetic conditions, and to devise an adaptive sampling strategy which is appropriate given that it is not possible to know *a priori* when the tracer will be mobilised nor where the tracer will be transported to[4]. This study adopted such an adaptive sampling strategy and the additional employment of (qualitative) UV torchlight surveys at night (during darkness) in the initial sampling campaigns enabled sampling locations to be targeted. The gradual dispersion of the tracer material along shore and continued presence of tracer material throughout the study also indicated that the study was not blown out and was effectively designed for the study area

The study has successfully addressed both of these important elements, and useful data has been collected on the nature of sediment transport on the beachface at Scarborough Bay.

4 The reality is that a bigger budget would translate into the deployment of a larger tracer volume which would create a larger initial signal which would persist longer through time; it would also facilitate collection and processing of a greater number of samples, including offshore samples where appropriate, which is a fundamental aspect contributing to the success of a tracer study. Less budgetary constraints can also open up the use of multiple tracer colours to label different source areas, an approach commonly used in field erosion studies.

Table 12: Details of the inshore wave climatology from the CCO Scarborough wave buoy through the dominant portion of the study (i.e. to 19th December, 2014)

Date	Wave Statistics			
	Average Wave Height (m)	Height Range (m)	Average Wave Period T (s)	Dominant Direction
5th- 6th December 2014	1.20	0.47 - 1.85	4.49	N
6th – 7th December 2014	0.58	0.44 - 0.77	3.09	SW - SE
7th – 8th December 2014	0.95	0.36 - 1.33	4.38	NW - NE
8th – 12th December 2014	1.23	0.58 - 2.43	4.39	N - SE
12th – 19th December 2014	1.26	0.57 - 2.82	5.18	N - NE

Both the magnetic susceptibility data (see Section 6.2) and early sampling activity showed that the first three inundation events (relatively small waves ~1.2 m, T~4.5 s) from the North mobilised and transported the tracer at the Deployment Zones in both northerly (~150 m) and southerly (~200 m) directions (Figure 13). In itself this indicates the magnitude and frequency of wave action that can drive beachface sand transport, and this type of information can be of use to beach managers interested in the threshold offshore events giving rise to sand transport.

The bi-directional transport is interesting from a number of perspectives. Firstly it would not ordinarily be expected that waves from the North would drive a *southward* longshore sand transport, and yet this is the information the study has revealed. Presumably the location and morphology of the headland and the sub-tidal bathymetry of the Bay is such that waves are refracted significantly as they enter the Bay to have a northward directed direction. The data also show that comparatively small waves (< 2 m) drive sand nearly half way to the West Pier / Lifeboat Station, which again may of a useful metric to beach managers.

That southerly sand transport is also observed suggests that this particular location, under the conditions experienced (Table 12), may be a zone of sediment transport divergence on the beachface, supplying sand (until depleted) in both directions. If this is the case, note the zone may move in response to differing wave climates possibly.

Sampling on the 7th and 8th December reveal continued transport in both northward and southward directs (Figure 14; Figure 15); northward tracer was found in the vicinity of the West Pier / Lifeboat station, indicating transport along the length of the beach in that direction. Southward transport was observed over similar distances (~600 m) towards the Cliff Railway. On the 7th this transport has occurred over a single additional tidal inundation. It is of interest to note that the waves were slightly *smaller* than the previous period (0.36 – 1.33 m; T=3-4 s), and yet are still driving sand transport on the beachface.

There is also evidence for some cross-shore (i.e. offshore directed) transport and cross shore gradients are seen in the tracer concentration data. It is also clear from the data that the rate of cross-shore transport is much lower than the rate of longshore transport.

On 12th December, tracer material has moved in northerly and southerly directions >500 metres (Figure 16). Tracer material is widely distributed and is present along much of the upper foreshore north and south of the deployment zones. Cross shore transport of the material has occurred [to a greater extent] south of the most southerly deployment zone and also seaward of the other two deployment zones. The waves during this time interval were largely from the north / northeast (for ~2 days), veering southeast and finally becoming westerlies for a few hours before returning to northerlies. The waves ranged in height from 0.58 – 2.43 m.

Of particular interest to the northern end of the beach, near the Lifeboat Station, tracer material is found in the middle and lower foreshore. This may indicate that once tracer material is deposited at the northerly extent of the beach, cross-shore transport moves the material towards the port entrance i.e. in an offshore direction as hypothesised in Section 1.1. Confirmation of this could have been achieved through sub-tidal sampling but such requires recurrent use of a vessel, higher level HSE considerations etc., which were beyond the budget of this project. However, it would be comparatively simple, using the methods and techniques employed here, to devise a simple study to assess further this potential sediment transport pathway using tracers.

By the 19th December the tracer signal is decreasing towards very low levels (Figure 17). Taken together with the data from 29th January, 2015, (Figure 18) it is clear that the tracer is spread widely over the beach-face but (although still visible to the eye) concentrations are very low (<13 g m^{-2}) including at the Deployment Zones. However, it is no longer possible to discern transport pathways, and the system is no longer being 'seeded' by the original source areas. The material present is firmly admixed with the native beach sediment.

6.2 Magnetic Susceptibility Data

The geologic parameter magnetic susceptibility parameter (χ_{LF}) can be a useful metric when using magnetic tracers to understand sediment transport. Whilst the tracer used exhibits a comparatively large signal:noise ratio (see Table 3) compared to wholly quartzitic mineral sand, on Scarborough beach specifically background magnetic susceptibility values were found to be higher than expected[5], and this limits the use of the magnetic susceptibility method in terms of delimiting downstream (alongshore) tracer/sediment transport. However, useful information is available on very nearfield tracer transport (loss of tracer) in the region at each deployment zone which enables a 'loss from source' type assessment to be made. Three magnetic susceptibility surveys were undertaken:

1. Before injection of the tracer (i.e. a background survey);
2. Post tracer injection; and
3. Post (initial) wave event (on 06/12/2014).

Table 13 presents the magnetic susceptibility data.

A mean (background) value for χ_{LF} prior to introduction of the tracer onto the beach face across the three injection zones is 134, which contrasts with that of 1004 following tracer introduction. The act of introducing the tracer into a trench therefore produces an approximately 9-fold over-concentration signal. Following the first wave event on 6th December, 2014, the surface χ_{LF} values decrease to typically < 200, and mean value across the three injection zones is 153. Figure 19 to 15 present this information graphically.

5 The reason for this is not known, but it may be related to ferrous anomalies in individual sand grains. Note, however, that a high susceptibility does not necessarily mean that a particle is magnetic, in the sense that it will adhere to a magnet upon exposure to a magnetic field.

Table 13: Raw magnetic susceptibility (χLF) values.

Sample	Magnetic Susceptibility (χ_{LF})		
	Back ground	Post tracer injection	Post event
Deployment Zone 1			
1	--	1223	119
2	328	1156	193
3	288	1038	141
4	166	1686	132
5	153	1135	131
6	189	1327	137
7	153	1392	231
8	164	944	89
9	119	1026	132
10	106	1256	106
Deployment Zone 2			
1	141	677	209
2	172	778	236
3	89	447	267
4	91	448	180
5	97	582	259
6	84	615	276
7	131	991	223
8	111	863	177
9	74	553	127
10	100	813	107

Sample	Magnetic Susceptibility (χLF)		
	Back ground	Post tracer injection	Post event
Deployment Zone 3			
1	196	1038	135
2	141	954	80
3	188	1162	84
4	146	1205	443
5	82	1093	69
6	100	1123	72
7	77	1159	66
8	51	1228	72
9	48	1138	56
10	43	1081	51

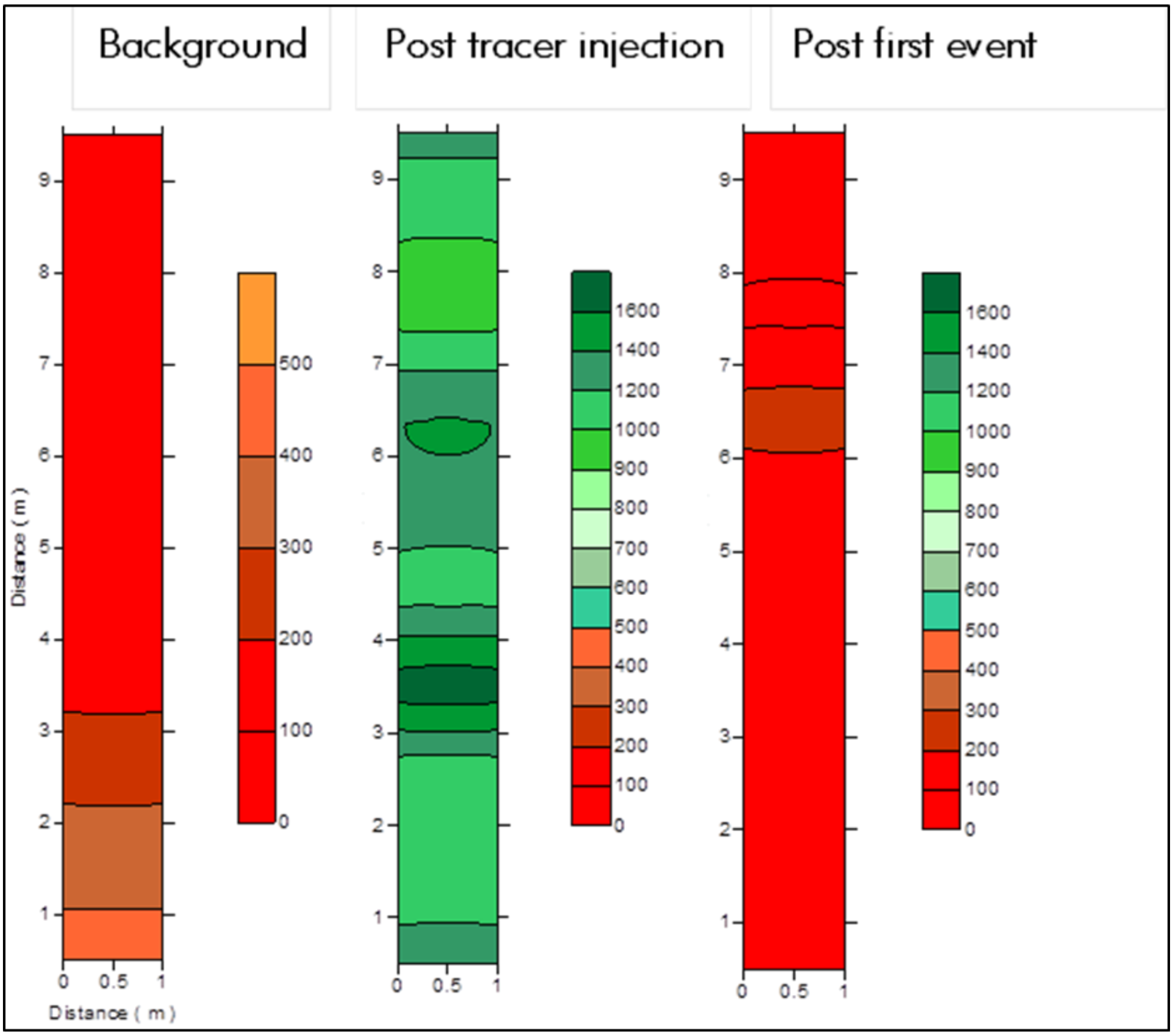

Figure 19. Distribution of surface low frequency magnetic susceptibility (χ_{LF}) at Deployment Zone 1 pre – injection of tracer (background), post injection of tracer and following the first wave event.

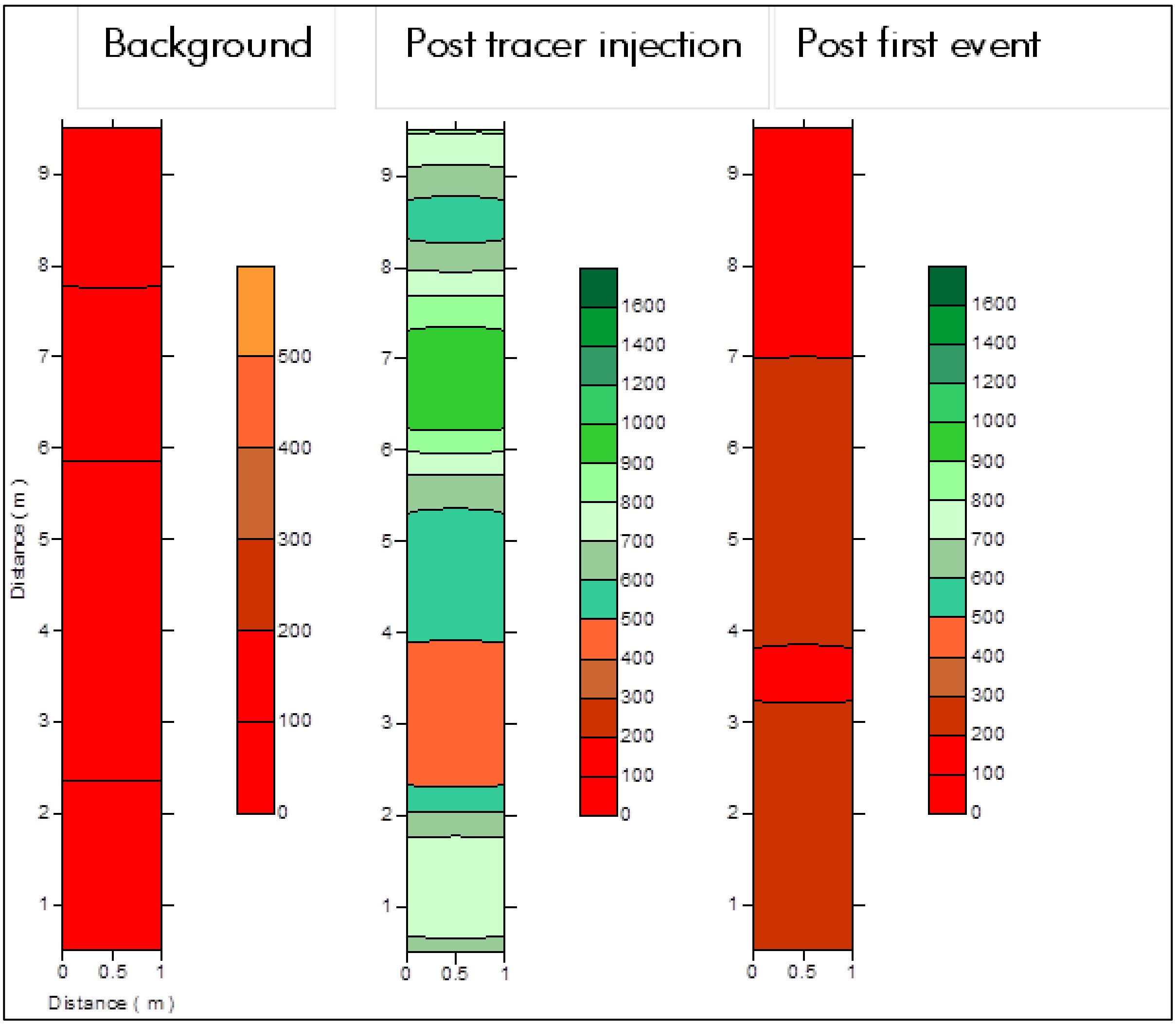

Figure 20. The low frequency magnetic susceptibility (χ_{LF}) of Deployment Zone 2 pre – injection of tracer (background), post injection of tracer and following the first wave event.

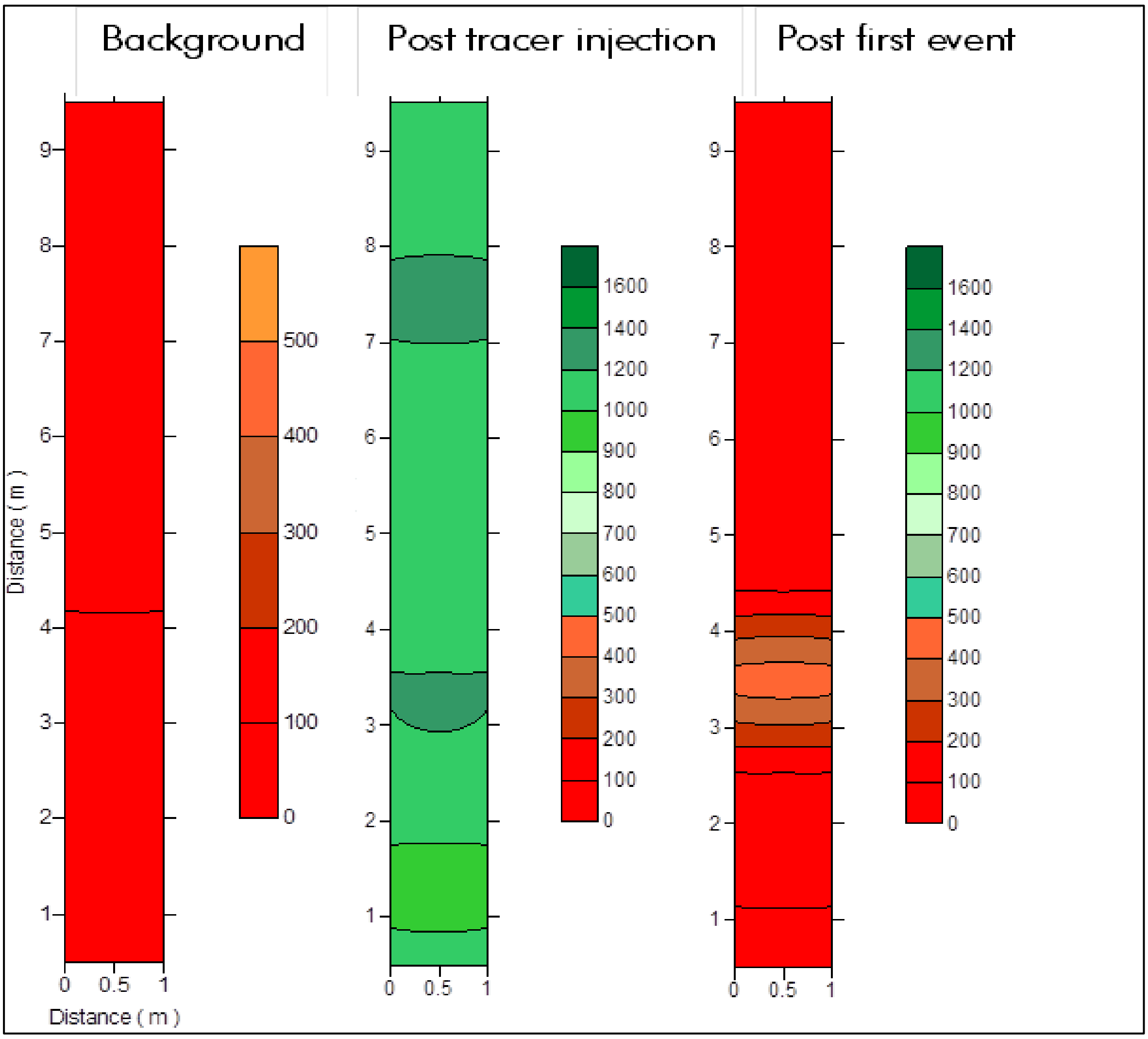

Figure 21. The low frequency magnetic susceptibility (χ_{LF}) of Deployment Zone 3 pre - injection of tracer (background), post injection of tracer and following the first wave event.

The magnetic susceptibility data are not calibrated i.e. a given value for K_{LF} cannot be related to a tracer mass density value (g m^{-2}). This can be readily undertaken if it is a specific requirement, but it was not done in this study. Thus, the data can be treated qualitatively only, and no transport rate information, which has units of mass per unit area per unit time, is available.

The data clearly indicate a substantial initial loss of tracer from the injection zone, with surface susceptibility values decreasing nearly to preceding background levels; on a qualitative level this means that the majority of the tracer was removed (transported) by the initial wave event and set in motion across the beachface. It is unfortunate that the background K_{LF} values at the site are so high (commonly values of ~5 – 10 maximum are observed for quartzitic UK beaches excepting areas of rich, hydraulically-equivalent placer deposits; see Table 3), and this precluded mapping of the ensuing dispersion of the tracer cloud by continued wave (and current) forcing using the susceptibility parameter.

7. CONCLUDING REMARKS

The aims of this study as outlined earlier were twofold:

(1) to test the postulated sediment transport pathways in Scarborough South Bay, and

(2) to test the use of these tracers as a valid method for future experiments of a similar nature.

(1) It is clear from the data collected during the sand tracking study that there is bi-directional movement of sand/sediment on the upper foreshore in South Bay, occurring in both southerly and northerly directions confirming the postulated transport pathways. This movement may simply be a response to the dominant prevailing direction of waves that impact upon the shore at any particular time. Additionally, we postulate that there may also be a local zone of sediment transport divergence on the beachface towards the north end of the Bay (in the area in front of the Grand Hotel), that is supplying sand (until depleted) in both directions. If this is the case, this zone may move (north or south) in response to differing wave climates.

(2) The data recorded during this study appears to confirm the northward direction of beach material toward the lifeboat station at the northern end of the Bay as indicated by numerical modelling. From the results of this study and others conducted by Partrac previously, as well as those studies in published literature, it is apparent that sediment tracing is a valuable tool in the sediment and coastal management arena. Tracing studies have the potential to improve upon the conceptual understanding of sediment transport regimes. They can be conducted to identify potential sediment source areas, transport pathways and areas of deposition and accumulation They also possess the unique ability to provide valuable checks and balances, using actual physical field data, for the calibration and validation (or not as the case may be) of the information gained from numerical modelling of sediment transport. Information that is all too often “taken as gospel” by scientists, consultants, managers and regulators alike. While sediment tracing is not a panacea for the management of sediment transport related problems and issues it is, we consider, a very useful “tool in the box”.

8. REFERENCES

Courtois G, and Monaco A (1969) Radioactive methods for the quantitative determination of coastal drift rate. Mar Geol 7:183 – 206.

Draaijer, A., Tadema Wielandt, R. and Houpt, P. M. 1984. Investigation on the applicability of fluorescent synthetic particles for the tracing of silt. Netherlands Organisation for Applied Scientific Research, Report R84/152 [in Dutch].

Guymer, I., Stovin, V.R., Gaskell, P., Maltby, L.L. and Pearson, J.M. (2010) Predicting The Deposition of Highway Derived sediments in a Receiving River Reach, 17th Congress of the Asia and Pacific Division (APD-IAHR), Auckland, New Zealand.

Heathershaw, A. D. and Carr, A. P. 1987. Measurements of sediment transport rates using radioactive tracers. In: Proceeding of the Coastal Sediments 1987 ASCE, New York, 399–412.

Forsyth, S.H., 2000 New developments in artificial fluorescent tracer counting techniques applied to sand transport studies. MSc. Thesis, University of Waikato, Hamilton, NZ. 42pp.

Inman, D.L. & Chamberlain, T.K. 1959. Tracing beach sand movement with irradiated quartz. 64, 41-47.

King, C. 1951. Depth of disturbance od sand on sea beaches by waves. Journal of Sedimentary Petrology, 21, 121-140.

Komar P.D. 1969. The longshore transport of sand on beaches. Unpublished PhD. Thesis University of California.

Louisse, C. J., Akkerman, R. J. and Suylen, J. M. 1986. A fluorescent tracer for cohesive sediment. In: International Conference on Measuring Techniques of Hydraulics Phenomena in Offshore, Coastal and Inland Waters. London, England, 9–11 April, 1986, 367–391.

Mccomb, P. J. and Black, K. P. 2005. Detailed observations of littoral transport using artificial sediment tracer in a high-energy, rocky-reef and iron sand environment. Journal of Coastal Research, 21, 358–373.

QEA. 2008. Lower Duwamish Waterway sediment transport modeling report. Prepared for Lower Duwamish Waterway Group. Quantitative Environmental Analysis, LLC, Montvale, NJ.

Sarma, T. P. & Iya, K. K. 1960. Preparation of artificial silt for tracer studies near Bombay Harbour. Journal Scientic Indeed Research India, Astrinli 19, 99–101.

Spencer, K., The2011 Development of rare earth element-labelled potassium-depleted clays for use as cohesive sediment tracers in aquatic environments. J Soils Sediments (paper in press).

Van Der Post, K. D., Oldfield, F. & Voulgaris, G. 1995. Magnetic tracing of beach sand: preliminary results. Coastal Dynamics '94, Proceedings of International Conference, 323–334.

Vila-concejo, A., Ferreira, O., Ciavola, P., Matias, A. & Dias, J. M. A. 2004. Tracer studies on the updrift margin of a complex inlet system. Marine Geology, 208, 43–72.

White, T., 1998 Status of measurement techniques for coastal sediment transport. Coastal Engineering, 35, 17-45.

9. APPENDIX I GILDEN PHOTONICS FLUOROSENS FLUORIMETER TECHNICAL SPECIFICATION

	SPECIFICATION
Optical Configuration	Right angle geometry, optical accessories for other geometries
Excitation Source	150W continuous Xenon Arc Lamp, Ozone Free
	200 to 2600nm spectral range
	XYZ bulb, rear mirror and lamp focus adjustments – factory pre-aligned
Monochromators	Czerny - Turner design
	300mm focal length
	Triple grating turret as standard
	Motorised continuously variable knife edge slits form 10µm to 3mm, as standard
	Stray Light performance 1:10 $^{-5}$
	Excitation Monochromator – blaze @ 300nm, 1200g/mm
	Emission Monochromator – blaze @ 500nm, 1200g/mm
Detector	185 – 670nm, blue sensitive singel photon counting photomultiplier. Dark count rate <100cps at room temperature
	185 – 870nm, red sensitive singel photon counting photomultiplier. Dark count rate <2000cps at room temperature
	185 – 1000nm, large area calirated Silicon Photodiode reference detector
	Optional InGaAs, InAs, InSb emission detectors for ranges into the NIR
Data Aquisition	100M counts per second photon counting system
	4 x 16 bit, 1Ms/s digitisers for analogue detectors and sample temperature monitor
	flexible user I/O port
Software	Operating System – WINDOWS®
	Exc, Em, Synchronous, Anisotropy, Ex-Em Mapping, Synchronous Mapping Spectra, 2D, 3D, and contour plotting
	Spectral Arithmetic, Normalisation, Smoothing, Differentiation, Integration, Spectral Conversion, Anisotropy Analysis (incl. G-factor correction)
Sensitivity	Water Raman signal-to-noise ration > 3000:1
	Excitation wavelength – 350nm, spectral bandwidth – 5nm, Integration Time = 1s

10. APPENDIX II TRACER DATA

Beach face samples		Sample position		Visual Description under Blue Light Illumination	Mass of Green Tracer per m^2 (g)
Sample Number	Date	Easting	Northing		
DZ01 - 01 - S1	06-Dec	504434.2	488232.0	4	51.3
DZ01 - 01 - S2	06-Dec	504434.2	488232.0	4	38
DZ01 - 01 - S3	06-Dec	504435.2	488231.7	4	44.6
DZ01 - 01 - S4	06-Dec	504436.5	488231.5	5	124.6
DZ01 - 01 - S5	06-Dec	504437.5	488231.4	5	75.3
DZ01 - 01 - S6	06-Dec	504438.7	488231.2	5	139.3
DZ01 - 01 - S7	06-Dec	504440.0	488230.9	5	103.3
DZ01 - 01 - S8	06-Dec	504441.2	488230.8	5	55.3
DZ01 - 01 - S9	06-Dec	504442.4	488230.6	5	128.6
DZ01 - 01 - S10	06-Dec	504443.5	488230.5	5	92.6
DZ02 - 01 - S01	06-Dec	504444.6	488230.4	5	769.9
DZ02 - 01 - S02	06-Dec	504441.5	488254.2	5	593.9
DZ02 - 01 - S03	06-Dec	504442.5	488254.1		457.9
DZ02 - 01 - S04	06-Dec	504443.6	488253.9	5	148.6
DZ02 - 01 - S05	06-Dec	504444.8	488253.7	5	151.3

Beach face samples		Sample position		Visual Description under Blue Light Illumination	Mass of Green Tracer per m^2 (g)
Sample Number	Date	Easting	Northing		
DZ01 - 01 - S1	06-Dec	504434.2	488232.0	4	51.3
DZ02 - 01 - S06	06-Dec	504445.9	488253.6	5	127.3
DZ02 - 01 - S07	06-Dec	504447.0	488253.3	5	171.3
DZ02 - 01 - S08	06-Dec	504447.9	488253.1	5	624.6
DZ02 - 01 - S09	06-Dec	504449.0	488252.8	5	47.3
DZ02 - 01 - S10	06-Dec	504450.2	488252.6	5	50
DZ03 - 01 - S01	06-Dec	504451.2	488252.4	2	39.3
DZ03 - 01 - S02	06-Dec	504488	488415.7	3	38
DZ03 - 01 - S03	06-Dec	504489.1	488415.2	5	0
DZ03 - 01 - S04	06-Dec	504490.3	488414.7	5	115.3
DZ03 - 01 - S05	06-Dec	504491.4	488414.2	5	70
DZ03 - 01 - S06	06-Dec	504492.3	488413.8	5	67.3
DZ03 - 01 - S07	06-Dec	504493.5	488413.4	5	72.6
DZ03 - 01 - S08	06-Dec	504494.5	488413.0	4	22.8
DZ03 - 01 - S09	06-Dec	504495.6	488412.5	4	47.3
DZ03 - 01 - S10	06-Dec	504496.7	488412.3	5	11.4
T-01-s01	06-Dec	504474.8	487987.3	3	11.4

Beach face samples		Sample position		Visual Description under Blue Light Illumination	Mass of Green Tracer per m^2 (g)
Sample Number	Date	Easting	Northing		
DZ01 - 01 - S1	06-Dec	504434.2	488232.0	4	51.3
T-01-s02	06-Dec	504465.3	488003.3	2	7.3
T-01-s03	06-Dec	504459.1	488022.1	2	0.7
T-01-s04	06-Dec	504453	488041.3	2	9.4
T-01-s05	06-Dec	504448.4	488060.4	3	0.7
T-01-s06	06-Dec	504444.6	488079.8	4	43.3
T-01-s07	06-Dec	504441.5	488099.8	3	40.6
T-01-s08	06-Dec	504438.3	488117.2	3	51.3
T-01-s09	06-Dec	504438.3	488135.3	3	48.6
T-01-s10 R1	06-Dec	504438.2	488153	3	48.6
T-01-s10 R2	06-Dec	504437.5	488171.7		Not analysed
T-01-s11 R1	06-Dec	504437.5	488171.7	5	74
T-01-s11 R2	06-Dec	504436.7	488191.7	5	80.6
T-01-s12 R1	06-Dec	504436.7	488191.7	5	54
T-01-s12 R2	06-Dec	504436.3	488210.3	5	72.6
T-01-s13 R1	06-Dec	504436.3	488210.3	5	68.6
T-01-s13 R2	06-Dec	504442.7	488263.7	5	95.3

Beach face samples		Sample position		Visual Description under Blue Light Illumination	Mass of Green Tracer per m^2 (g)
Sample Number	Date	Easting	Northing		
DZ01 - 01 - S1	06-Dec	504434.2	488232.0	4	51.3
T-01-s14 R1	06-Dec	504442.7	488263.7	5	80.6
T-01-s14 R2	06-Dec	504446.5	488281.4	4	71.3
T-01-s15	06-Dec	504446.5	488281.4	2	39.3
T-01-S15 R1	06-Dec	504446.5	488281.4	5	48.6
T-01-S15 R2	06-Dec	504450.1	488299.1	4	62
T-01-s16	06-Dec	504450.1	488299.1	5	107.3
T-01-s17	06-Dec	504454.8	488315.6	3	50
T-01-s18	06-Dec	504459.2	488331	5	40.6
T-01-s19	06-Dec	504465.8	488346.8	4	16.6
T-01-s20	06-Dec	504474.2	488361.9	4	52.6
T-01-s21	06-Dec	504478	488384.7	4	7.3
T-01-s22	06-Dec	504483.6	488401.9	2	7.3
T-01-s23	06-Dec	504491.3	488422.7	5	144.6
T-01-s24	06-Dec	504495.8	488437.9	3	35.3
T-01-s25	06-Dec	504503.5	488454.1		Not analysed
T-01-s26	06-Dec	504508.6	488472.5	5	71.3

Beach face samples		Sample position		Visual Description under Blue Light Illumination	Mass of Green Tracer per m^2 (g)
Sample Number	Date	Easting	Northing		
DZ01 - 01 - S1	06-Dec	504434.2	488232.0	4	51.3
T-01-s27 R1	06-Dec	504517.7	488489.6	3	39.3
T-01-s27 R2	06-Dec	504526.9	488506.5	4	51.3
T-01-s28	06-Dec	504526.9	488506.5	4	36.6
T-01-s29	06-Dec	504535.1	488523.3	3	35.3
T-01-s30	06-Dec	504544.8	488541.2	3	9.4
LF01-s01	07-Dec	504783.5	488600.4	1	0.3
LF01-s02	07-Dec	504753.2	488574.8	0	0
LF01-s03	07-Dec	504724.2	488547.8	1	1.5
LF01-s04	07-Dec	504697.3	488519.5	0	0
LF01-s05	07-Dec	504673	488488	0	0
LF01-s06	07-Dec	504653.1	488454.8	1	1.5
LF01-s07	07-Dec	504637	488420	0	0
LF01-s08	07-Dec	504621.4	488383.6	1	0.3
LF01-s09	07-Dec	504608.7	488346.1	1	1.5
LF01-s10	07-Dec	504594.4	488310.1	0	0
LF01-s11	07-Dec	504585.7	488281.2	1	2.9

Beach face samples		Sample position		Visual Description under Blue Light Illumination	Mass of Green Tracer per m^2 (g)
Sample Number	Date	Easting	Northing		
DZ01 - 01 - S1	06-Dec	504434.2	488232.0	4	51.3
LF01-s12	07-Dec	504580.8	488242.2	0	0
LF01-s13	07-Dec	504578	488202.9	0	0
LF01-s14	07-Dec	504576.4	488163.4	1	0.3
LF01-s15	07-Dec	504579	488125.6	2	0.7
LF01-s16	07-Dec	504582.8	488089.3	1	0.3
LF01-s17	07-Dec	504586.7	488052.3	0	0
LF01-s18	07-Dec	504596.4	488016	1	0.3
LF01-s19	07-Dec	504604.1	487979.8	1	0.3
LF01-s20	07-Dec	504613.5	487942.7	1	0.3
LF01-s21	07-Dec	504622.1	487905.6	1	1.5
LF01-s22	07-Dec	504629.8	487859.8	1	0.3
LF01-s23	07-Dec	504647.7	487748.6	1	11.4
MF01-s01	07-Dec	504581.1	487726.8		Not analysed
MF01-s02	07-Dec	504569.8	487762		Not analysed
MF01-s03	07-Dec	504558.9	487797.1	0	0
MF01-s04	07-Dec	504549.2	487832.5	1	7.3

Beach face samples		Sample position		Visual Description under Blue Light Illumination	Mass of Green Tracer per m^2 (g)
Sample Number	Date	Easting	Northing		
DZ01 - 01 - S1	06-Dec	504434.2	488232.0	4	51.3
MF01-s05	07-Dec	504540.4	487869.3	1	9.4
MF01-s06	07-Dec	504533	487906.5	1	0.3
MF01-s07	07-Dec	504525.6	487946.9	2	0.7
MF01-s08	07-Dec	504509.6	487980.6	1	0.3
MF01-s09	07-Dec	504497.6	488016.3	2	0.7
MF01-s10	07-Dec	504490.6	488051.4	3	8.4
MF01-s11	07-Dec	504483.4	488087.7	4	7.3
MF01-s12	07-Dec	504478.6	488124.5	5	67.3
MF01-s13	07-Dec	504475	488200.4	3	35.3
MF01-s13 dup					Not analysed
MF01-s14	07-Dec	504480	488241.2	2	7.3
MF01-s15	07-Dec	504490.8	488278.2	1	0.3
MF01-s16	07-Dec	504497.3	488314.7	0	0
MF01-s17	07-Dec	504504.6	488351.6	0	0
MF01-s18	07-Dec	504514.3	488387	0	0
MF01-s19	07-Dec	504523.6	488418.6	1	0.3

Beach face samples		Sample position		Visual Description under Blue Light Illumination	Mass of Green Tracer per m^2 (g)
Sample Number	Date	Easting	Northing		
DZ01 - 01 - S1	06-Dec	504434.2	488232.0	4	51.3
MF01-s20	07-Dec	504538.8	488450.2	0	0
MF01-s21	07-Dec	504557.6	488481.3	1	9.4
MF01-s22	07-Dec	504578.1	488512.9	0	0
MF01-s23	07-Dec	504599.2	488543.5	0	0
MF01-s24	07-Dec	504623.7	488572.9	1	0.3
MF01-s25	07-Dec	504649.7	488599.6	1	0.3
MF01-s26	07-Dec	504675.3	488623.4	1	0.3
MF01-s27	07-Dec	504733.4	488673.3	0	0
UF01-s01	07-Dec	504693.4	488709.5	2	0.7
UF01-s02	07-Dec	504670.6	488689.3	1	0.3
UF01-s03	07-Dec	504643.3	488670.4	4	7.3
UF01-s04	07-Dec	504621.4	488653.2	2	9.4
UF01-s05	07-Dec	504602.9	488633.8		Not analysed
UF01-s06	07-Dec	504586.3	488611	3	15.6
UF01-s07	07-Dec	504569.5	488588.9	5	25.9
UF01-s08	07-Dec	504553.2	488564.9	4	50

Beach face samples		Sample position		Visual Description under Blue Light Illumination	Mass of Green Tracer per m^2 (g)
Sample Number	Date	Easting	Northing		
DZ01 - 01 - S1	06-Dec	504434.2	488232.0	4	51.3
UF01-s09	07-Dec	504540.6	488540.7	3	15.6
UF01-s10	07-Dec	504527.4	488515	4	36.6
UF01-s11	07-Dec	504516	488489.3	3	21.7
UF01-s12	07-Dec	504505.4	488465.1	5	43.3
UF01-s13	07-Dec	504495.4	488440.7	4	46
UF01-s14	07-Dec	504489.7	488416	5	309.9
UF01-s15	07-Dec	504482.4	488390.2	1	0.3
UF01-s16	07-Dec	504474.5	488363.9	5	42
UF01-s17	07-Dec	504465.1	488334.9	4	56.6
UF01-s18	07-Dec	504456	488308	4	46
UF01-s19	07-Dec	504449.4	488282.3	5	60.6
UF01-s20	07-Dec	504445	488252.5	5	272.6
UF01-s21	07-Dec	504440.2	488230.3	5	192.6
UF01-s22	07-Dec	504438.6	488202.7	5	76.3
UF01-s23	07-Dec	504439	488173.1	5	66
UF01-s24	07-Dec	504439.9	488146.9	4	54

Beach face samples		Sample position		Visual Description under Blue Light Illumination	Mass of Green Tracer per m^2 (g)
Sample Number	Date	Easting	Northing		
DZ01 - 01 - S1	06-Dec	504434.2	488232.0	4	51.3
UF01-s25	07-Dec	504440.4	488120.4	3	13.5
UF01-s26	07-Dec	504442.6	488094.5	3	35.3
UF01-s27	07-Dec	504445.6	488069.8	4	38
UF01-s28	07-Dec	504450.3	488034.7	3	0.7
UF01-s29	07-Dec	504457.1	488009.6	2	7.3
UF01-s30	07-Dec	504471.9	487986.5	3	35.3
UF01-s31	07-Dec	504481	487960.4	2	7.3
UF01-s32	07-Dec	504486.4	487931.3	2	0.7
UF01-s33	07-Dec	504490.3	487904.5	1	7.3
UF01-s34	07-Dec	504496.8	487872.7	1	38
UF01-s35	07-Dec	504505.8	487847.1	1	0.3
UF01-s36	07-Dec	504514.6	487819.1	5	11.4
UF01-s37	07-Dec	504520.1	487792.3	0	0
UF01-s38	07-Dec	504524.3	487761.8	1	0.3
UF01-s39	07-Dec	504529.9	487735.2	1	6.3
UF01-s40	07-Dec	504534	487707.8	1	12.5

Beach face samples		Sample position		Visual Description under Blue Light Illumination	Mass of Green Tracer per m^2 (g)
Sample Number	Date	Easting	Northing		
DZ01 - 01 - S1	06-Dec	504434.2	488232.0	4	51.3
UF02-s01	08-Dec	504692.8	488708.5	1	0.3
UF02-s02	08-Dec	504668.9	488692.1	2	11.4
UF02-s03	08-Dec	504646.5	488674.7	4	7.3
UF02-s04	08-Dec	504624.7	488657	3	38
UF02-s05	08-Dec	504603	488636.4	3	42
UF02-s06	08-Dec	504584.7	488615.9	4	43.3
UF02-s07	08-Dec	504567.6	488593.4	5	10.4
UF02-s08	08-Dec	504553.5	488567.3	5	32
UF02-s09	08-Dec	504539.6	488542.7	4	46
UF02-s10	08-Dec	504527	488517.3	4	24.8
UF02-s11	08-Dec	504515.8	488489.9	5	60.6
UF02-s12	08-Dec	504506.1	488463.2	3	39.3
UF02-s13	08-Dec	504497.2	488436.6	2	0.7
UF02-s14	08-Dec	504488.8	488410.4	2	35.3
UF02-s15	08-Dec	504480.3	488383.4	3	10.4
UF02-s16	08-Dec	504472.5	488357	5	64.6

Beach face samples		Sample position		Visual Description under Blue Light Illumination	Mass of Green Tracer per m^2 (g)
Sample Number	Date	Easting	Northing		
DZ01 - 01 - S1	06-Dec	504434.2	488232.0	4	51.3
UF02-s17	08-Dec	504464.1	488330.5	4	22.8
UF02-s18	08-Dec	504457.7	488302.4	3	40.6
UF02-s19	08-Dec	504451.4	488275.3	3	90
UF02-s20	08-Dec	504447	488248.1	5	86
UF02-s21	08-Dec	504444.9	488219.2	5	114
UF02-s22	08-Dec	504442	488192.1	5	87.3
UF02-s23	08-Dec	504440.9	488163.9		Not analysed
UF02-s24	08-Dec	504442.9	488136.3		Not analysed
UF02-s25	08-Dec	504445	488108.6	3	35.3
UF02-s26	08-Dec	504448.5	488080.7	2	7.3
UF02-s27	08-Dec	504452.1	488052.7	3	7.3
UF02-s28	08-Dec	504458.1	488025.4	2	9.4
UF02-s29	08-Dec	504471.6	488000.2	2	1.5
UF02-s30	08-Dec	504483.3	487974.7	2	7.3
UF02-s31	08-Dec	504489.3	487947.5	2	7.3
UF02-s32	08-Dec	504495.1	487922	2	7.3

Beach face samples		Sample position		Visual Description under Blue Light Illumination	Mass of Green Tracer per m^2 (g)
Sample Number	Date	Easting	Northing		
DZ01 - 01 - S1	06-Dec	504434.2	488232.0	4	51.3
UF02-s33	08-Dec	504500.1	487894.3	1	7.3
UF02-s34	08-Dec	504514.2	487837.2	2	0.8
RA01-s01	08-Dec	504443	488240.5	5	114
RA01-s02	08-Dec	504452.7	488225	5	92.6
RA01-s03	08-Dec	504461.6	488208.6	3	9.4
RA01-s04	08-Dec	504473.4	488194.3	3	7.3
RA01-s05	08-Dec	504486.9	488181.7	1	0.3
RA01-s06	08-Dec	504501.6	488170.2	1	0.3
RA01-s07	08-Dec	504515.8	488158.9	2	7.3
RA01-s08	08-Dec	504531	488147.5	1	2.9
RA01-s09	08-Dec	504520.9	488131.3	3	11.4
RA01-s10	08-Dec	504505.2	488120.2	4	7.3
RA01-s11	08-Dec	504485	488151.8	3	38
RA01-s12	08-Dec	504485	488151.8	2	0.7
RA01-s13	08-Dec	504475	488167.5	2	35.3
RA01-s14	08-Dec	504465.1	488183.2	5	14.5

Beach face samples		Sample position		Visual Description under Blue Light Illumination	Mass of Green Tracer per m^2 (g)
Sample Number	Date	Easting	Northing		
DZ01 - 01 - S1	06-Dec	504434.2	488232.0	4	51.3
RA01-s15	08-Dec	504455.5	488199.3	5	20.7
RA01-s16	08-Dec	504438.9	488219.5	5	96.6
RA01-s17	08-Dec	504452.1	488232.7	5	76.6
RA01-s18	08-Dec	504470	488232.1	3	9.4
RA01-s19	08-Dec	504487.7	488230	2	3.6
RA01-s20	08-Dec	504505.6	488228.2	1	10.4
RA01-s21	08-Dec	504523.5	488226.2	1	7.3
RA01-s22	08-Dec	504541.9	488224.1	1	0.3
RA01-s23	08-Dec	504560.2	488222.2	0	0
RA01-s24	08-Dec	504563.1	488241.1		Not analysed
RA01-s25	08-Dec	504545.2	488243	0	0
RA01-s26	08-Dec	504527	488244.6	1	7.3
RA01-s27	08-Dec	504508.8	488247.1	0	0
RA01-s28	08-Dec	504490.5	488249.4	1	1.5
RA01-s29	08-Dec	504472.2	488253		Not analysed
RA01-s30	08-Dec	504459.5	488265.9	3	39.3

Beach face samples		Sample position		Visual Description under Blue Light Illumination	Mass of Green Tracer per m^2 (g)
Sample Number	Date	Easting	Northing		
DZ01 - 01 - S1	06-Dec	504434.2	488232.0	4	51.3
RA01-s31	08-Dec	504476.1	488274.4		Not analysed
RA01-s32	08-Dec	504492.8	488281.9	1	0.3
RA01-s33	08-Dec	504509.1	488290.6	0	0
RA01-s34	08-Dec	504524.7	488298.8	1	0.3
RA01-s35	08-Dec	504540.9	488309.2	1	0.3
RA01-s36	08-Dec	504523.8	488330.5	1	0.3
RA01-s37	08-Dec	504509.6	488320.1		Not analysed
RA01-s38	08-Dec	504495.5	488307.6	0	0
RA01-s39	08-Dec	504479	488294.6	2	1.5
RA01-s40	08-Dec	504461.6	488282.2	1	0.3
RA01-s41	08-Dec	504483.2	488324.5	1	0.3
RA01-s42	08-Dec	504500.7	488331.7	1	0.3
RA01-s43	08-Dec	504491.4	488348.1	1	0.3
RA01-s44	08-Dec	504516.8	488342.7	1	1.5
RA01-s45	08-Dec	504543.2	488346.8	1	0.3
RA01-s46	08-Dec	504530.8	488361.2	0	0

Beach face samples		Sample position		Visual Description under Blue Light Illumination	Mass of Green Tracer per m^2 (g)
Sample Number	Date	Easting	Northing		
DZ01 - 01 - S1	06-Dec	504434.2	488232.0	4	51.3
RA01-s47	08-Dec	504519.4	488374.1	0	0
RA01-s48	08-Dec	504507.8	488387.1	1	0.3
RA01-s49	08-Dec	504497.9	488398.7	1	1.5
RA01-s50	08-Dec	504499.3	488415.4	4	35.3
RA01-s51	08-Dec	504513.4	488410.3	0	0
RA01-s52	08-Dec	504530.8	488403.9	1	9.4
RA01-s53	08-Dec	504547.7	488399.2	1	2.9
RA01-s54	08-Dec	504565.4	488393.7	0	0
RA01-s55	08-Dec	504573.2	488426.1	0	0
RA01-s56	08-Dec	504554.9	488422.7	0	0
RA01-s57	08-Dec	504536.6	488419.1		Not analysed
RA01-s58	08-Dec	504518	488420.7	3	1.5
RA01-s59	08-Dec	504512.6	488430.1	2	2.9
RA01-s60	08-Dec	504527.3	488438.2	2	0.7
RA01-s61	08-Dec	504543.7	488446.5		Not analysed
RA01-s62	08-Dec	504558.1	488453.2	0	0

Beach face samples		Sample position		Visual Description under Blue Light Illumination	Mass of Green Tracer per m^2 (g)
Sample Number	Date	Easting	Northing		
DZ01 - 01 - S1	06-Dec	504434.2	488232.0	4	51.3
RA01-s63	08-Dec	504574.7	488462.2	0	0
RA01-s64	08-Dec	504590.8	488471.2	0	0
RA01-s65	08-Dec	504611	488509.4	0	0
RA01-s66	08-Dec	504585.1	488499.5	0	0
RA01-s67	08-Dec	504568	488491.9	1	30
RA01-s68	08-Dec	504550.5	488484.6	0	0
RA01-s69	08-Dec	504533.2	488477.4	1	30
RA01-s70	08-Dec	504530.6	488489.7	2	70
RA01-s71	08-Dec	504544.6	488501.8	1	30
RA01-s72	08-Dec	504558.9	488514	0	0
RA01-s73	08-Dec	504572.7	488526.8		Not analysed
RA01-s74	08-Dec	504587.4	488538.7	1	360
RA01-s75	08-Dec	504580.1	488556.7	1	30
RA01-s76	08-Dec	504566.6	488543.3	1	30
UF03-s01	12-Dec	504691.4	488702.2		Not analysed
UF03-s02	12-Dec	504667.6	488688.3	2	1.5

Beach face samples		Sample position		Visual Description under Blue Light Illumination	Mass of Green Tracer per m^2 (g)
Sample Number	Date	Easting	Northing		
DZ01 - 01 - S1	06-Dec	504434.2	488232.0	4	51.3
UF03-s03	12-Dec	504646.5	488668.9	2	0.7
UF03-s04	12-Dec	504630.6	488651.8	1	7.3
UF03-s05	12-Dec	504608.4	488629.1	2	0.7
UF03-s06	12-Dec	504591.2	488608.6	2	11.4
UF03-s07	12-Dec	504573.5	488584.9	2	7.3
UF03-s08	12-Dec	504559	488563.4		Not analysed
UF03-s09	12-Dec	504544	488539.7	2	0.7
UF03-s10	12-Dec	504530.8	488514.9		Not analysed
UF03-s11	12-Dec	504518.4	488489	3	1.5
UF03-s12	12-Dec	504508	488459.8	5	1.5
UF03-s13	12-Dec	504498.3	488429.5		Not analysed
UF03-s14	12-Dec	504489.8	488400.4		Not analysed
UF03-s15	12-Dec	504481.9	488376.9	3	7.3
UF03-s16	12-Dec	504474.8	488343.3	3	11.4
UF03-s17	12-Dec	504465.8	488308.6	2	43.3
UF03-s18	12-Dec	504456.6	488283.9	2	7.3

Beach face samples		Sample position		Visual Description under Blue Light Illumination	Mass of Green Tracer per m^2 (g)
Sample Number	Date	Easting	Northing		
DZ01 - 01 - S1	06-Dec	504434.2	488232.0	4	51.3
UF03-s19	12-Dec	504444.3	488251.3	5	2.9
UF03-s20	12-Dec	504441.7	488224.6	3	36.6
UF03-s21	12-Dec	504439	488200	3	12.5
UF03-s22	12-Dec	504439.7	488170	4	9.4
UF03-s23	12-Dec	504439	488141	3	39.3
UF03-s24	12-Dec	504442.2	488114.4	2	7.3
UF03-s25	12-Dec	504446.1	488085.5		Not analysed
UF03-s26	12-Dec	504450	488057.8		Not analysed
UF03-s27	12-Dec	504457.8	488031.2	2	1.5
UF03-s28	12-Dec	504470.1	488005.9	2	0.7
UF03-s29	12-Dec	504478.6	487977.2		Not analysed
UF03-s30	12-Dec	504485.8	487947.3	2	0.7
LF02-s01	12-Dec	504552.2	487948.8	0	0
LF02-s02	12-Dec	504546.2	487984.3	1	0.3
LF02-s03	12-Dec	504542.6	488025.4		Not analysed
LF02-s04	12-Dec	504539.1	488063.1	1	0.3

Beach face samples		Sample position		Visual Description under Blue Light Illumination	Mass of Green Tracer per m^2 (g)
Sample Number	Date	Easting	Northing		
DZ01 - 01 - S1	06-Dec	504434.2	488232.0	4	51.3
LF02-s05	12-Dec	504537.1	488096.5	2	3.6
LF02-s06	12-Dec	504534.9	488136.5	2	0.8
LF02-s07	12-Dec	504540.6	488172.3	1	2.9
LF02-s08	12-Dec	504546.2	488210.2	0	0
LF02-s09	12-Dec	504551.3	488246	1	0.3
LF02-s10	12-Dec	504558.2	488285.1	1	0.3
LF02-s11	12-Dec	504567.8	488322	0	0
LF02-s12	12-Dec	504580	488357.9		Not analysed
LF02-s13	12-Dec	504592.8	488395	1	1.5
LF02-s14	12-Dec	504607.1	488427.6	1	4.3
LF02-s15	12-Dec	504625.2	488462.5	0	0
LF02-s16	12-Dec	504643.3	488495.2	0	0
LF02-s17	12-Dec	504666.1	488524.6	0	0
LF02-s18	12-Dec	504690.9	488551.9	0	0
LF02-s19	12-Dec	504717	488577	1	0.3
LF02-s20	12-Dec	504745.8	488601	1	0.3

Beach face samples		Sample position		Visual Description under Blue Light Illumination	Mass of Green Tracer per m^2 (g)
Sample Number	Date	Easting	Northing		
DZ01 - 01 - S1	06-Dec	504434.2	488232.0	4	51.3
LF02-s21	12-Dec	504775.3	488620.6	1	0.3
MF02-s01	12-Dec	504739	488671	0	0
MF02-s02	12-Dec	504705.6	488649.1	1	7.3
MF02-s03	12-Dec	504672.3	488622.7	1	1.5
MF02-s04	12-Dec	504644.3	488596.5	0	0
MF02-s05	12-Dec	504614.4	488565.8	0	0
MF02-s06	12-Dec	504590.8	488540.7	0	0
MF02-s07	12-Dec	504573.9	488510.3	1	0.3
MF02-s08	12-Dec	504557.7	488477.6	1	0.3
MF02-s09	12-Dec	504542.1	488448.3	1	0.3
MF02-s10	12-Dec	504526.7	488411.3	3	2.9
MF02-s11	12-Dec	504513.7	488378.7	1	0.3
MF02-s12	12-Dec	504498.2	488346.1	1	0.3
MF02-s13	12-Dec	504491.3	488306.9	1	2.9
MF02-s14	12-Dec	504483	488270	2	7.3
MF02-s15	12-Dec	504480.6	488231	2	0.7

Beach face samples		Sample position		Visual Description under Blue Light Illumination	Mass of Green Tracer per m^2 (g)
Sample Number	Date	Easting	Northing		
DZ01 - 01 - S1	06-Dec	504434.2	488232.0	4	51.3
MF02-s16	12-Dec	504476.2	488194.2	3	9.4
MF02-s17	12-Dec	504472.5	488156.2	4	13.5
MF02-s18	12-Dec	504474.1	488118.4	3	17.6
MF02-s19	12-Dec	504480.8	488079.6	3	2.9
MF02-s20	12-Dec	504489.5	488042	2	1.5
MF02-s21	12-Dec	504496.9	488003.2	2	Not analysed
MF02-s22	12-Dec	504508.8	487964.5	1	0.3
T02-s01	12-Dec	504525.3	487984.9	1	0.3
T02-s02	12-Dec	504522.5	488022.7	1	1.5
T02-s03	12-Dec	504522.9	488059.4	1	1.5
T02-s04	12-Dec	504522.1	488097.3	1	0.3
T02-s05	12-Dec	504521.3	488134	2	0.7
T02-s06	12-Dec	504524.4	488168.5	2	4.3
T02-s07	12-Dec	504529.4	488206.5		Not analysed
T02-s08	12-Dec	504536.9	488247.9	1	1.5
T02-s09	12-Dec	504544.5	488284.8	1	2.2

Beach face samples		Sample position		Visual Description under Blue Light Illumination	Mass of Green Tracer per m² (g)
Sample Number	Date	Easting	Northing		
DZ01 - 01 - S1	06-Dec	504434.2	488232.0	4	51.3
T02-s10	12-Dec	504553.4	488323.9	0	0
T02-s11	12-Dec	504565	488357.6	0	0
T02-s12	12-Dec	504576.5	488396.8	0	0
T02-s13	12-Dec	504590.1	488429.4	1	0.3
T02-s14	12-Dec	504607.4	488468.8	1	0.3
T02-s15	12-Dec	504624.9	488503.7	0	0
T02-s16	12-Dec	504645	488536.4	0	0
T02-s17	12-Dec	504667.1	488568.1	0	0
T02-s18	12-Dec	504694.5	488593.2	1	2.9
T02-s19	12-Dec	504723.3	488615	0	0
T02-s20	12-Dec	504752.9	488633.5	0	0
T03-s01	12-Dec	504707.2	488664.7	0	0
T03-s02	12-Dec	504675.8	488640.6		Not analysed
T03-s03	12-Dec	504644.4	488619.9	0	0
T03-s04	12-Dec	504612.4	488593.5	1	0.3
T03-s05	12-Dec	504587.1	488559.6	1	0.3

Beach face samples		Sample position		Visual Description under Blue Light Illumination	Mass of Green Tracer per m^2 (g)
Sample Number	Date	Easting	Northing		
DZ01 - 01 - S1	06-Dec	504434.2	488232.0	4	51.3
T03-s06	12-Dec	504566.4	488527.9	1	0.3
T03-s07	12-Dec	504551.5	488495.3	1	0.3
T03-s08	12-Dec	504532.2	488454.8	1	1.5
T03-s09	12-Dec	504519.3	488420	5	7.3
T03-s10	12-Dec	504503.8	488387.4	1	0.3
T03-s11	12-Dec	504492.8	488352.6		Not analysed
T03-s12	12-Dec	504481.9	488316.7	1	9.4
T03-s13	12-Dec	504474.3	488280.9	2	6.5
T03-s14	12-Dec	504467.9	488244.1	2	0.7
T03-s15	12-Dec	504459.7	488203.8	4	16.6
T03-s16	12-Dec	504457.4	488164.8	4	11.4
T03-s17	12-Dec	504457.5	488132.5	4	12.5
T03-s18	12-Dec	504460.2	488098.1	3	17.6
T03-s19	12-Dec	504459.2	488056.9	2	1.5
T03-s20	12-Dec	504469.1	488021.5	1	1.5
LF-01	19-Dec	504566.6	487981.9	0	0

Beach face samples		Sample position		Visual Description under Blue Light Illumination	Mass of Green Tracer per m^2 (g)
Sample Number	Date	Easting	Northing		
DZ01 - 01 - S1	06-Dec	504434.2	488232.0	4	51.3
LF-02	19-Dec	504564.7	488016.7	0	0
LF-03	19-Dec	504561.5	488051.2	1	1.5
LF-04	19-Dec	504560.3	488085.4	1	0.3
LF-05	19-Dec	504558.7	488120	3	5.1
LF-06	19-Dec	504559	488156	3	0.7
LF-07	19-Dec	504559.3	488192.9	2	1.5
LF-08	19-Dec	504561.7	488228.2	1	0.3
LF-09	19-Dec	504565.7	488263.5	1	2.2
LF-10	19-Dec	504572.9	488299	0	0
LF-11	19-Dec	504583.5	488334.5	1	0.3
LF-12	19-Dec	504595.4	488369.3		Not analysed
LF-13	19-Dec	504609.1	488406.6	1	0.3
LF-14	19-Dec	504622.7	488440.6	0	0
LF-15	19-Dec	504637.9	488473.5	0	0
LF-16	19-Dec	504656.3	488502.6	0	0
LF-17	19-Dec	504679.4	488531.1	0	0

Beach face samples		Sample position		Visual Description under Blue Light Illumination	Mass of Green Tracer per m^2 (g)
Sample Number	Date	Easting	Northing		
DZ01 - 01 - S1	06-Dec	504434.2	488232.0	4	51.3
LF-18	19-Dec	504704.7	488556.7	1	0.3
LF-19	19-Dec	504731.4	488580.6	0	0
LF-20	19-Dec	504759	488603.3	0	0
LF-21	19-Dec	504791.3	488622	0	0
MF-01	19-Dec	504754.9	488671.4	0	0
MF-02	19-Dec	504725.7	488651.1	0	0
MF-03	19-Dec	504696.3	488628.8	4	Not analysed
MF-04	19-Dec	504667.4	488605.7	0	0
MF-05	19-Dec	504641.7	488580.3	0	0
MF-06	19-Dec	504617.1	488551.2		Not analysed
MF-07	19-Dec	504596.8	488522.2	0	0
MF-08	19-Dec	504580.4	488491.4	0	0
MF-09	19-Dec	504563.9	488457.7	1	0.3
MF-10	19-Dec	504550.8	488425	2	0.7
MF-11	19-Dec	504539.9	488391.9	2	7.3
MF-12	19-Dec	504527.9	488359.7	0	0

Beach face samples		Sample position		Visual Description under Blue Light Illumination	Mass of Green Tracer per m^2 (g)
Sample Number	Date	Easting	Northing		
DZ01 - 01 - S1	06-Dec	504434.2	488232.0	4	51.3
MF-13	19-Dec	504516	488326.9	0	0
MF-14	19-Dec	504507.6	488292.5	2	5.1
MF-15	19-Dec	504500.1	488258.2	2	0.7
MF-16	19-Dec	504493.7	488223.2	2	1.5
MF-17	19-Dec	504491.9	488186.7	3	Not analysed
MF-18	19-Dec	504494.5	488148.8	3	0.7
MF-19	19-Dec	504497.7	488111.5	3	1.5
MF-20	19-Dec	504501.1	488075.1	2	0.7
MF-21	19-Dec	504504.2	488038	1	0.3
MF-22	19-Dec	504511.6	487982	1	0.3
UF-01	19-Dec	504491.3	487883.6	1	0.3
UF-02	19-Dec	504487	487912.1	1	7.3
UF-03	19-Dec	504483.3	487941.6	2	1.5
UF-04	19-Dec	504476.9	487972.2	2	Not analysed
UF-05	19-Dec	504464.3	487999.7	1	0.3
UF-06	19-Dec	504454	488027.2	1	0.3

Beach face samples		Sample position		Visual Description under Blue Light Illumination	Mass of Green Tracer per m^2 (g)
Sample Number	Date	Easting	Northing		
DZ01 - 01 - S1	06-Dec	504434.2	488232.0	4	51.3
UF-07	19-Dec	504448.8	488055.5	2	7.3
UF-08	19-Dec	504445.9	488088.6	2	0.7
UF-09	19-Dec	504444.1	488119.1	1	4.3
UF-10	19-Dec	504441.8	488149.4	3	6.3
UF-11	19-Dec	504441.9	488180.4	3	35.3
UF-12	19-Dec	504440.1	488212.9	2	7.3
UF-13	19-Dec	504443.2	488241.5	3	7.3
UF-14	19-Dec	504449.4	488269.2		Not analysed
UF-15	19-Dec	504457.2	488297.6	1	10.4
UF-16	19-Dec	504464.7	488327.9	1	13.5
UF-17	19-Dec	504472.6	488359.6	2	7.3
UF-18	19-Dec	504482.5	488389.1	2	7.3
UF-19	19-Dec	504492.7	488418.6	1	0.3
UF-20	19-Dec	504502.7	488447.1	1	9.4
UF-21	19-Dec	504513.8	488474	1	7.3
UF-22	19-Dec	504526.2	488500.1	1	0.3

Beach face samples		Sample position		Visual Description under Blue Light Illumination	Mass of Green Tracer per m^2 (g)
Sample Number	Date	Easting	Northing		
DZ01 - 01 - S1	06-Dec	504434.2	488232.0	4	51.3
UF-23	19-Dec	504540	488526.5	1	1.5
UF-24	19-Dec	504556	488551.4	1	0.3
UF-25	19-Dec	504572.5	488575.1		Not analysed
UF-26	19-Dec	504594.3	488603.8	0	0
UF-27	19-Dec	504614.2	488625.9	1	2.9
UF-28	19-Dec	504635.7	488645.7	0	0
UF-29	19-Dec	504664.8	488670.3	2	10.4
UF-30	19-Dec	504693.8	488694	1	0.3
UF6-01	29-Jan	54.28339	0.3935	1	0.8
UF6-02	29-Jan	54.28311	0.394083	0	0
UF6-02 R2	29-Jan	54.28311	0.394083	0	0
UF6-03	29-Jan	54.28283	0.394556	2	7.3
UF6-04	29-Jan	54.28247	0.395083	2	0.7
UF6-05	29-Jan	54.28214	0.395528	2	0.7
UF6-06	29-Jan	54.28167	0.395944	2	0.7
UF6-07	29-Jan	54.28117	0.396417	2	6.3

Beach face samples		Sample position		Visual Description under Blue Light Illumination	Mass of Green Tracer per m^2 (g)
Sample Number	Date	Easting	Northing		
DZ01 - 01 - S1	06-Dec	504434.2	488232.0	4	51.3
UF6-08	29-Jan	54.28072	0.396583	2	7.3
UF6-09	29-Jan	54.28033	0.396833	2	7.3
UF6-10	29-Jan	54.27989	0.397111	2	7.3
UF6-11	29-Jan	54.27925	0.397472	2	1.5
UF6-12	29-Jan	54.27881	0.397444	2	7.3
UF6-13	29-Jan	54.27836	0.397472	2	7.3
UF6-14	29-Jan	54.27786	0.397528	2	0.7
UF6-15	29-Jan	54.2775	0.397472	2	0.7
UF6-16	29-Jan	54.27703	0.397417	1	0.8
UF6-17	29-Jan	54.27453	0.396667		Not analysed
MF6-01	29-Jan	54.28314	0.393139	0	0
MF6-02	29-Jan	54.28289	0.393694	1	0.3
MF6-03	29-Jan	54.28256	0.394167	1	0.3
MF6-04	29-Jan	54.28225	0.394667	1	9.4
MF6-05	29-Jan	54.28192	0.395083	1	6.3
MF6-06	29-Jan	54.2815	0.395528	1	0.8

Beach face samples		Sample position		Visual Description under Blue Light Illumination	Mass of Green Tracer per m^2 (g)
Sample Number	Date	Easting	Northing		
DZ01 - 01 - S1	06-Dec	504434.2	488232.0	4	51.3
MF6-07	29-Jan	54.28106	0.395972	1	0.8
MF6-08	29-Jan	54.28067	0.39625	2	7.3
MF6-09	29-Jan	54.28025	0.3965	1	6.3
MF6-10	29-Jan	54.27986	0.396667	1	0.3
MF6-11	29-Jan	54.27919	0.396972	1	0.3
MF6-12	29-Jan	54.27878	0.397056	1	7.3
MF6-13	29-Jan	54.27831	0.396917	2	0.7
MF6-14	29-Jan	54.27789	0.396944	2	7.3
MF6-15	29-Jan	54.2775	0.397056	1	1.5
MF6-16	29-Jan	54.27708	0.396889	1	0.3
MF6-17	29-Jan	54.27656	0.396944	1	7.3
MF6-18	29-Jan	54.27581	0.396583	1	0.3
MF6-19	29-Jan	54.27525	0.39625	0	0
MF6-20	29-Jan	54.27469	0.396	1	0.3